TRYM ALLAN JENOFTSEN
SUPERVISOR: EDUARDO ALEXANDRE BARROS E SILVA

Assessing Cadmium's Impact on Lymphatic Endothelial Cell's Health

Bachelor Thesis Spring 2024

Biological Chemistry

Department of Chemistry, Bioscience, and Environmental Engineering

Faculty of Science and Technology

Acknowledgement

First of all, I would like to thank my supervisor Eduardo Silva for his support and encouragement throughout this thesis. He has been more than willing to answer all my questions and understandably formulated and visualized his answers.

I would like to dedicate a special thanks to Kristine Wighus Holtmon. She has been there for me and with me through thick and thin. We have spent countless hours together at the lab working on our theses. She has also been a good and important friend to me throughout my three years studying biological chemistry.

I want to thank Katrine Kirkeby, Anette Idland, Sarah Ravndal, Eivind Eie, and Lars Bustad for holding out with me through our three years of studying together. You have been the best of friends to me, and I do not think my time studying in Stavanger would have been the same without you.

I want to thank my friends in Trondheim, you know who you are, for always being there when I have questions or struggle with different problems. I could not have asked for a better friend group, and I am glad I have you.

Lastly, I want to express my gratitude toward my family which has been supportive and believed in me. You have been a source of strength for me throughout this thesis, and you have always encouraged me to do my best.

Abstract

Cadmium (Cd) is a hazardous heavy metal which presents adverse concerns towards public and environmental health, primarily through its cytotoxic and carcinogenic properties (1). In this thesis, the impact of Cd on lymphatic endothelial cells (LECs) was investigated as few to no current studies have been published on this topic. It is essential to get an understanding of how LECs are affected by Cd. They are one of the main structural and functional components of the lymphatic system, and the lymphatic system is an important part of the immune and circulatory systems (2). *In vitro* proliferation assays and *in vitro* 3D fibrin gel microcarrier sprouting assays were conducted to assess how Cd affected the cell viability, proliferation and sprouting of Dermal Lymphatic Adult Human Microvascular Endothelial Cells (HMVEC-dLyAd). The results obtained in this thesis should be looked at critically, but similar observations have been reported in different endothelial cells exposed to Cd in prior studies (3). The results suggest that Cd has cytotoxic and anti-lymphangiogenic properties, negatively affecting cell viability, proliferation and sprouting. Ultimately, more research is necessary to uncover the complex molecular mechanisms of how Cd affects LECs, but this thesis serves as an important starting point.

Table of Contents

List of Figures

List of Tables

Abbreviations

Cd: Cadmium

HMVEC: Human Microvascular Endothelial Cell

HMVEC-dLyAd: Dermal Lymphatic Adult Human Microvascular Endothelial Cell

HUVEC: Human Umbilical Vein Endothelial Cell

LEC: Lymphatic Endothelial Cell

MCs: Microcarriers

1. Introduction

1.1. Heavy Metals

Heavy metals play a significant role in environmental contamination and pose a severe threat to human health and ecosystems due to their persistence and bioaccumulation (4, 5). Heavy metals are metals with a density higher than 5 g/cm^3, they are found naturally in the earth's crust and can be released into the environment through natural and anthropogenic sources (5, 6). The most common heavy metals are lead, mercury, arsenic and cadmium (5). Heavy metals frequently react with biological systems by forming cations with a high affinity towards the nucleophilic sites of vital macromolecules. The disruption of these macromolecules can cause several acute and chronic symptoms like vascular damage, kidney and gastrointestinal dysfunction, nervous system disorders, skin lesions, immune system dysfunction, birth defects, and cancer (4, 5). Heavy metals can severely impact soil, water bodies and ecosystems through pollution. Heavy metals bioaccumulate in plants and aquatic organisms, and over time the higher organisms will develop high concentrations of these heavy metals due to their prolonged biological half-life (7) (see Figure 1).

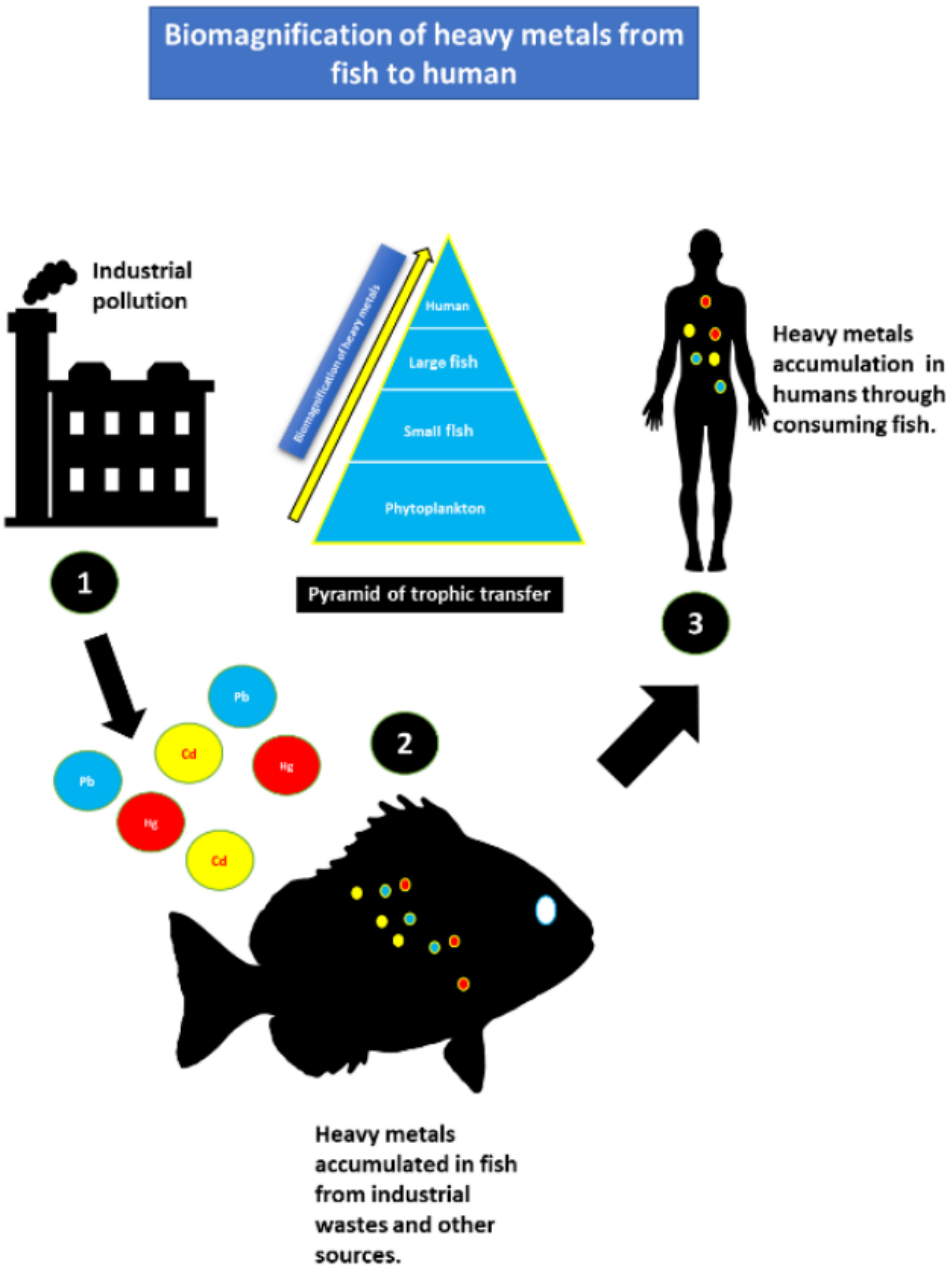

Figure 1. Release of industrial heavy metals in aquatic systems and bioaccumulation of heavy metals (Retrieved from (8)).

The adverse health effects caused by heavy metal pollution are extensively documented, and it is a staggering physical and psychological burden for the affected (9). This also represents a considerable economic burden for affected individuals who need treatment and is a substantial economic burden for societies, potentially costing up to 10 % of the global GDP which amounts to 10 trillion US $ (10). Given the widespread presence and high abundance of heavy metals, governments have implemented various measures to reduce heavy metal's impact on the environment. By establishing maximum permissible emission limits, there has been a

drastic reduction in heavy metal pollution (11). Additionally, remediation techniques are implemented to remove heavy metals from contaminated areas. Phytoremediation, where plants are used to extract heavy metals from soil and water is the most common technique and it is cost-effective (12).

1.2. Cadmium

Cadmium (Cd), a hazardous heavy metal, presents significant health and environmental concerns globally. Cd's inherent toxicity necessitates a more comprehensive understanding of its impact on human health. Cd is listed as number seven on the Agency for Toxic Substances and Disease Registry's (ATSDR) substance priority list, which is a list that ranks substances based on their toxicity, frequency, and potential for human exposure (13). Cd is listed as element number 48 on the periodic table. Additionally, it is found naturally in the earth's crust at a concentration of 0.1-0.5 ppm and is commonly found in zinc, lead, and copper ores (14, 15). Cd is highly prevalent in the environment due to natural and anthropogenic sources. Natural sources of Cd are volcanic emissions, weathering of rocks, forest fires, hydrothermal vents, airborne soil particles, and meteoric dust, where soil particles are the primary source (16). Anthropogenic sources are the main sources of Cd-contamination in the environment, including the production and use of inorganic fertilizers, combustion of fossil fuel, mining, smelting, and refining of non-ferrous metals, and other industrial activities (15, 17).

Cd from the atmosphere enters the soil and accumulates in plants (17). Plants such as moss and lichens which have no connection to the soil absorb atmospheric Cd (18). The most common way people are exposed to Cd is by oral ingestion, where around 0.5 to 8% of the Cd is absorbed depending on its solubility. In the gastrointestinal tract, Cd binds non-specifically to anionic sites on the membrane, followed by a rate-limiting internalisation which is temperature dependent (19, 20). However, when smoking tobacco approximately 40 to 60 % of the Cd gets absorbed through the lungs entering our vascular system (21). Other sources of Cd exposure are inexpensive jewellery, toys and plastics, especially for children, however many countries have banned Cd in such products (22). Cd has a biological half-life ranging from 16-30 years in the human body, and the World Health Organization (WHO) recommends not exceeding Cd intake of 60-70 µg/day for adults. Due to the prolonged biological half-life of Cd in the body, the majority of people are at risk for developing high concentrations of Cd throughout life. However, those employed in industries which produce or utilize Cd are at the greatest risk of developing cadmium poisoning. Additionally, smokers represent the second

highest risk group (23). Approximately 1.2 billion people out of 8.1 billion are tobacco users, and typically have Cd blood levels and body burdens over than double that of nonsmokers, putting more than 1.2 billion people at increased risk of developing Cd poisoning, and other implications (23-25).

High concentrations of Cd in certain foods, particularly in Norway, pose significant public health concerns, prompting authorities to issue advisories against the consumption of fish and shellfish from specific regions due to industrial activity (26-28). In 2009 and 2012, calculations of Cd intake from the diet were conducted by the European Food Safety Authority (EFSA), which indicated that cadmium intake in Europe falls within the range of tolerable weekly intake (TWI), set to 2.5 μg/kg body weight. On behalf of these calculations, EFSA has concluded that there is a need to reduce Cd exposure in the population. The Cd intake in Norway is approximately the same as in Europe, but some parts of the population may be more exposed, especially regions which regularly consume brown crab meat or offal from domestic and wild animals (28). In Norway crab, reindeer, moose, sheep, scallops and oysters have incredibly high concentrations of Cd as depicted in Figure 2, the Norwegian Scientific Committee for Food and Environment (VKM) reported that brown crab meat north of Salten fjord had a mean value of 11 200 μg Cd/kg wet weight (ww) (see Figure 2) (26).

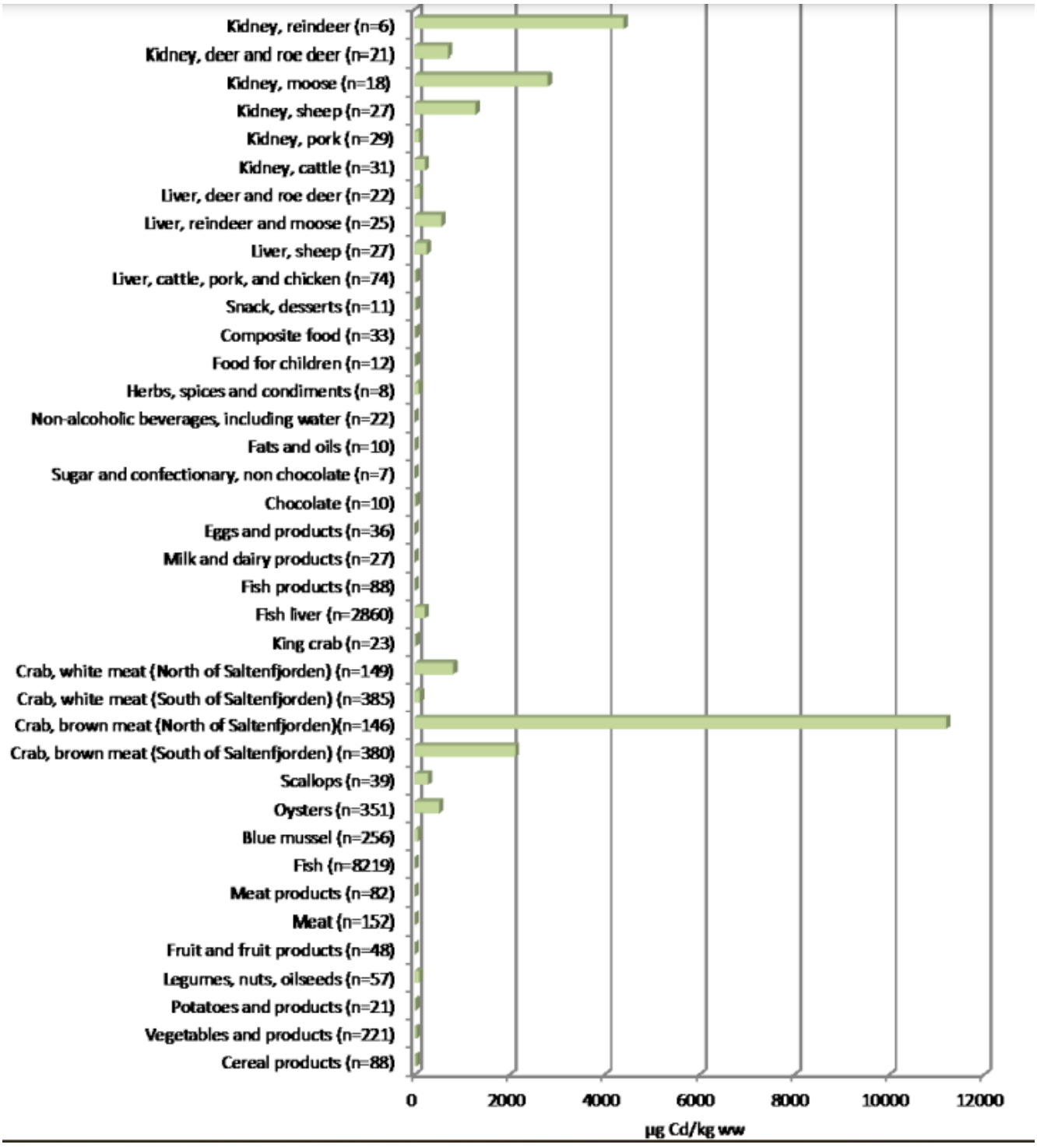

Figure 2: Overview of food products, and the concentration of Cadmium (Retrieved from (29)).

These high concentrations in certain foods pose a public health risk to the Norwegian population. Therefore the authorities have advised against consuming fish and shellfish from several fjords, lakes and ports, especially where there is industrial activity (27, 30). Cd is known to cause various human diseases such as cancer, kidney issues, and vascular diseases.

Cd-poisoning has been recorded worldwide and it is one of the global health problems that affects several different organs and in some cases deaths. A compelling example of the severe symptoms of cadmium poisoning is the historic Itai Itai "ouch ouch" disease from the Toyama Prefecture in Japan. It is known that Cd affects the bone. Victims of Cd-poisoning had severe osteoporosis and osteomalacia resulting in the development of soft fragile bones as depicted in Figure *3*. The osteomalacia and osteoporosis caused excruciating pain so severe that the term "Itai Itai" (it hurts, it hurts) was given to describe it (31, 32). Renal dysfunctions were also observed as Cd predominantly accumulates in the kidneys and liver. Renal dysfunction is characterised by tubular lesions, proteinuria, and calcium loss, which lead to malabsorption of nutrients, further worsening their conditions (31). In severe cases of Itai Itai disease, renal anaemia is observed due to insufficient production of erythropoietin in the kidneys (33).

Figure 3. Bone structure caused by Itai Itai disease (Retrieved from (34)).

Studies show that Cd can induce endothelial dysfunction *in vitro* and accelerate atherosclerotic plaque formation *in vivo*. Atherosclerosis is characterised by the gradual buildup of plaque in the artery walls, leading to narrowing and hardening. Atherosclerosis often causes symptoms such as heart attack or strokes (35). In cultured human umbilical vein endothelial cells (HUVECs) exposed to Cd, there were increased membrane permeability, growth inhibition, necrosis, and DNA strand breaks (36). The mechanisms of Cd-promotion of atherosclerosis indirectly increase reactive oxygen species (ROS) by replacing iron and copper in the cytoplasmic and membrane proteins. The free iron and copper ions undergo

Fenton reactions, increasing the oxidative stress (37). However, the effects Cd have on the lymphatic system are less studied and understood, but no less important considering its role in immunity and cardiovascular health.

1.3. The Lymphatic System

The lymphatic system is one of the important components of the circulatory system, immune system, and metabolic system, regulating fluid homeostasis, fat absorption, and the enhancement and facilitation of the immune system (38). The lymphatic system consists of lymphatic vessels, lymphatic cells, and lymphatic fluid. In humans, the primary lymphoid organs are the bone marrow, thymus, and fetal liver. Lymphocytes are derived from stem cells in the bone marrow, stem cells destined to become B-cells stay in the bone marrow while those destined to become T-cells migrate to the thymus where they undergo maturation. Mature B and T-cells exit the primary lymphoid organs and are transported by the vascular system to secondary lymphoid organs like lymph nodes, the spleen, Peyer's patches (PPs), and mucosal lymphoid tissues (39, 40). As blood circulates, blood plasma leaks into tissues through the thin capillary walls. This interstitial fluid contains oxygen, glucose, amino acids, and other essential nutrients. Most of the interstitial fluid leaks back into the bloodstream, but a fraction of the fluid remains in the tissue and is transported by the lymphatic system back to the bloodstream (41). The lymphatic vasculature is composed of networks of lymphatic vessels that resemble a tree-like structure, with smaller branches converging into larger vessels (42).

1.3.1. Lymphatic Endothelial Cells (LECs)

One of the most important components of the lymphatic system is LECs. They are a specialized subset of endothelial cells that form the structure of the lymphatic vasculature, including lymph nodes and lymph vessels (43). The lymphatic vascular tree consists of three parts, the lymphatic capillaries, the pre-collectors, and the collecting lymphatics as illustrated in Figure 4. LECs located at the lymphatic capillaries have discontinuous "button-like" junctions, which border valve-like openings serving as routes of immune cell, lipid, and macromolecule transportation from the interstitial space (44). While the button-like junctions allow reabsorption of interstitial fluid, it would not be possible without the structure created from anchoring junctions between LECs and the Extra Cellular Matrix (ECM). When fluid

accumulates in the interstitial space the pressure increases, this causes the filaments that anchor LECs to the ECM to pull on the valve-like openings. This opens the valve-like openings, allowing interstitial fluid to travel through (44, 45). LECs located in the collecting lymphatics vessels have tight "zipper-like" junctions, which prevent leakage, supporting the unidirectional flow of lymph back to the bloodstream (43).

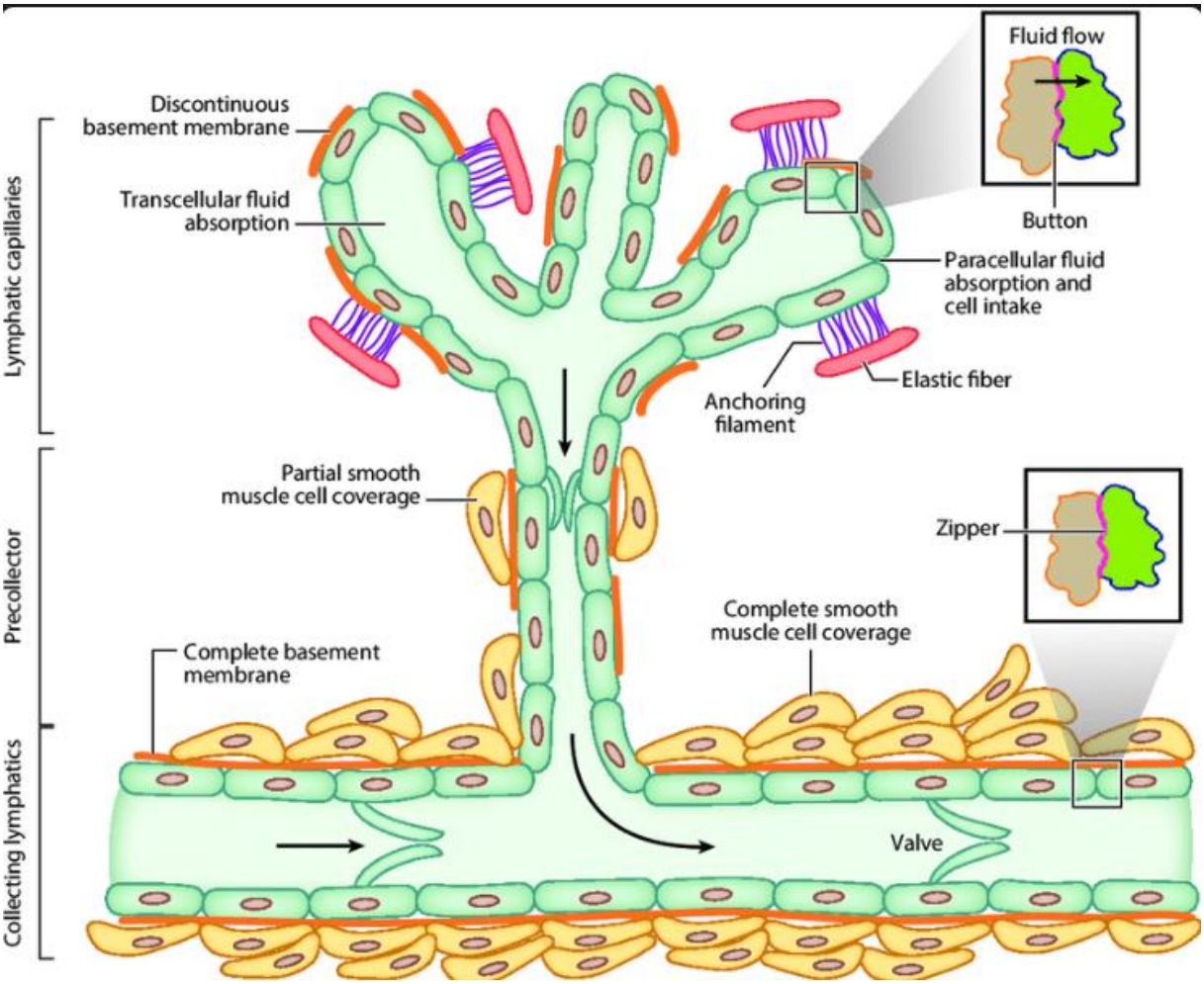

Figure 4. Illustration of the lymphatic vascular tree (Retrieved from (46)).

During inflammatory stimulus LECs secrete chemokines to recruit immune cells to the lymph nodes, where immune cells can be activated and undergo clonal expansion, initiating an adaptive immune response (47). If the LECs are dysfunctional this can lead to lymphedema, impairing lymphatic drainage and immune cell trafficking, causing swelling in the local region, and negatively affecting the immune response (48). Lymphangiogenesis is often seen during lymphedema (49).

1.3.2. Lymphangiogenesis

Lymphangiogenesis is a term used to describe the growth and development of new lymphatic vessels from pre-existing lymphatic vessels (50). Lymphangiogenesis is far less studied than angiogenesis, which is the growth and development of new blood vessels from pre-existing ones (51, 52). The study of lymphangiogenesis became more relevant when its role in cancer development was discovered (50). Lymphangiogenesis occurs during embryonic development approximately two weeks after the cardiovascular system (53). Post-developmental lymphangiogenesis occurs during pathological conditions such as wound healing, inflammation, and tumorigenesis. A common feature in these conditions is tissue edema, which increases the demand for fluid drainage and immune cell trafficking (54). Similar to angiogenesis, lymphangiogenesis also has tip cells as the leading cells of a sprout followed by stalk cells (55, 56). A Sprout is a multicellular structure with a length of at least 150 µm (57).

The process of lymphangiogenesis is induced by extracellular signals from growth factors, such as Vascular Endothelial Growth Factor C (VEGF-C) and Vascular Endothelial Growth Factor D (VEGF-D). VEGF-C and VEGF-D bind to the Vascular Endothelial Growth Factor Receptor family member VEGFR-3 (55). VEGFR-3 can be viewed as the master receptor of lymphangiogenesis, studies on VEGFR-3 knockout mice resulted in cardiovascular failure. Mice with VEGF-$C^{-/-}$ genotype were found to have endothelial cells (ECs) differentiate into LECs, but these cells were unable to sprout and form lymph vessels (58). The same study showed that the transcription factor Prospero Homeobox 1 (Prox1) serves as a master "switch" in determining LEC fate (58). How Prox1 and other transcription factors regulate cell adhesion and cytoskeleton dynamics, which are essential for lymphangiogenesis remains unresolved (55, 58).

1.4. *In Vitro* Models for Studying Lymphangiogenesis.

In vitro models are essential tools for studying lymphangiogenesis as they provide a highly controlled environment to study molecular and cellular mechanisms underlying lymphangiogenesis. Different phases of lymphangiogenesis can be assessed such as proliferation, sprouting and tube formation, this level of control is difficult to achieve in the advanced *in vivo* setting (59, 60).

1.4.1. Proliferation assay

In vitro proliferation assays are valuable models for studying cell proliferation, which is an essential part of lymphangiogenesis, cytotoxicity, and cell viability to monitor the health and response of a cell culture after treatment of certain stimuli (61).

There are several different types of proliferation assays which analyse different aspects of proliferation and metabolism, and fluorescently label cells to determine viability (61). The one conducted in this thesis is a simple Trypan blue cell counting proliferation assay. The principle of this *in vitro* proliferation assay is to seed cells in six-well plates and expose them to certain concentrations of Cd, then after a given time, the cells are stained with Trypan blue and the viable/non-viable cells are counted and cell viability is determined. Trypan blue passes through the porous cell membrane of dead cells and enters the cytoplasm, the intact cell membrane of live cells blocks Trypan blue from entering the cytoplasm, distinguishing between live and dead cells (62).

The advantages of using six-well plates in proliferation assays are the low costs, equal growth surface area, and reduced variability compared to smaller well sizes (24 and 96-well plates), and it is already widely used to determine cytotoxic effects in the pharmaceutical industry (63-65). Advantages of Trypan blue staining and hemocytometer cell counting is a direct and quantitative measure of viable/non-viable cells by manually counting them, and it is relatively cheap (61, 66).

Disadvantages of this assay are that it is a 2D *in-vitro* assay, which is different from the *in-vivo* environment, it is not suited for high-throughput applications compared to smaller wells and rapid cell counts, the accuracy of the cell counting can also be affected by cell clumping making it hard to accurately determine the cell number or uneven distribution, and lastly, this method is prone to a lot of possible human error (67).

Overall 2D proliferation assay is a valuable tool for studying the effects of different stimuli on LEC proliferation. The data provided from these assays give important insights but should be complemented by other *in vitro* or *in vivo* models to gain a more comprehensive understanding of the biology and function of LECs (68).

1.4.2. 3D Fibrin Gel Microcarrier Sprouting Assay

3D fibrin gel microcarrier assay is a well-established method for studying the angiogenesis/lymphangiogenesis of different endothelial cells. The fibrin gel resembles the *in vivo* environment of LECs, providing a more physiologically relevant environment than the 2D proliferation assay (69).

The principle of this assay is that LECs are seeded onto microcarriers (MCs) and then embedded within a 3D fibrin gel. The LECs then sprout out from the MCs, mimicking the early stages of lymphatic vessel formation (70). The advantages of this assay are the structural similarity between the gel and *in vivo* environment, and the MCs coated with the LECs create an equivalent to an established vessel in vivo (71, 72). Compared to 2D culture assays this method presents a more physiologically relevant assessment of LEC behaviour and response to different stimulants (73).

However, the 3D assay does have some limitations. It is technically challenging to conduct, and it is more expensive than a 2D proliferation assay (72). The 3D gel provides a more complex environment than the 2D assays, but it still doesn't fully replicate the complexity of the *in vivo* environment as it lacks several other cell types and ECM components (72). Additionally, there is always the risk of human errors, which could influence the results (74).

Overall the 3D fibrin gel assay is a valuable model for studying how different stimuli affect lymphangiogenesis in a more physiologically relevant context compared to 2D culture systems (75).

1.5. Knowledge Gap

There are extensive studies conducted on Cd's adverse effects on human health, most studies focus on its impact on the lungs and kidneys, and on HUVECs and Human Microvascular Endothelial Cells (HMVECs) (3). In contrast, the lymphatic system's response to cadmium is less understood as there are few to no current studies where HMVEC-dLyAd have been exposed to Cd. Additionally, the process and mechanisms of angiogenesis are extensively studied and understood, compared to lymphangiogenesis (55).

1.6. Objectives

This thesis aims to investigate how Cd affects the proliferation and sprouting of LECs. There is extensive research on how Cd affects HUVECs and HMVECs, but not on HMVEC-dLyAd (3). Due to Cd being abundant in the Norwegian and European diets, acquiring a wider understanding of how Cd impacts different cell types is critical. The LECs are one of the main functional and structural components of the lymphatic system and LEC dysfunction can lead to lymphedema and other implications regarding the immune response (76).

2. Methods

2.1. Preparation of Microvascular Endothelial Growth Medium-2 (EGM™-2MV Medium)

Before preparation, all external surfaces were decontaminated with diluted ethanol (70%), VWR). The contents of Microvascular Endothelial Cell Growth Medium SingleQuots™ supplements (EGM™-2 Singlequotes™ kit) (Lonza, #CC-4147) were thawed, decontaminated with ethanol (70%), and transferred to Endothelial Cell Growth Basal Medium-2 (EBM™-2 Medium) (Lonza, #CC-3156), inside the biosafety cabinet (Thermo scientific). To get as much content from each vial, they were rinsed with the medium. EGM™-2 Singlequotes™ kit contains 0.5 ml human Epidermal Growth Factor (hEGF), 0.5 ml Vascular Endothelial Growth Factor (VEGF), 0.5 ml R3-Insulin-like Growth Factor-1 (R3-IGF-1), 0.5 ml Ascorbic Acid, 0.2 ml Hydrocortisone, 2.0 ml human Fibroblast Growth Factor-Beta (hFGF-B), 10 ml Fetal Bovine Serum (FBS) and 0.5 ml Gentamicin/Amphotericin-B (GA-1000).

2.2. *In Vitro* Sub-Culture of Lymphatic Endothelial Cells

A T-75 flask (VWR) was marked with name, cell type, passage nr, and date. The T-75 flask was decontaminated with ethanol (70 %) and placed in the biosafety cabinet before adding 10 ml media. A cryovial with HMVEC-DLyAd P6 was retrieved from the liquid nitrogen tank and decontaminated with ethanol (70 %) before briefly twisting the cap to relieve pressure, and then retightening, it inside the biosafety cabinet. The cryovial were placed in a water bath (37 °C) for no longer than 2 minutes. Before adding the cells to the T-75 flask the content of the cryovial was titrated up and down a few times then up and down in the flask, to ensure optimal transfer of cells. The culture vessel was then rocked gently in a figure-eight motion and incubated at 37 °C with 5% CO_2, and 90% humidity.

After 19 hours the medium was aspirated, and a new 10 ml was added. Then this process was repeated every 48 hours until the cells were 70-80 % confluent and ready for passage or cryopreservation.

To detach the cells 7 ml trypsin (Corning, #25-053-CI) was thawed and then allowed to reach room temperature. Two new T-75 flasks were marked with cell type, passage number, name and date, then 18 ml media was thawed and transferred to each flask, so they each contained 9 ml. In the culture flask media was aspirated, 2 ml trypsin was added, and the culture flask was rocked in a figure-eight motion, the trypsin was removed after approximately 30 seconds.

Then 5 ml trypsin was added before incubating for 5 minutes at 37 °C. After 5 minutes the flask was placed under a microscope to check if the cells were detached. The trypsin in the flask was then neutralized by 5 ml media and this time it was poured on the side where the cells had been growing. The cells were transferred to a 15 ml centrifugate tube (VWR) and centrifuged at 200 G for 5 minutes (Kubota 2800). The supernatant mix was aspirated, and 2 ml media were added to the tube, then 1 ml was transferred to each new culture flask creating HMVEC-Lymph P7 cultures. The media was changed after 22 hours then every 48 hours until the cells were 70% confluent. A simplified visual overview of this process is illustrated in Figure 5.

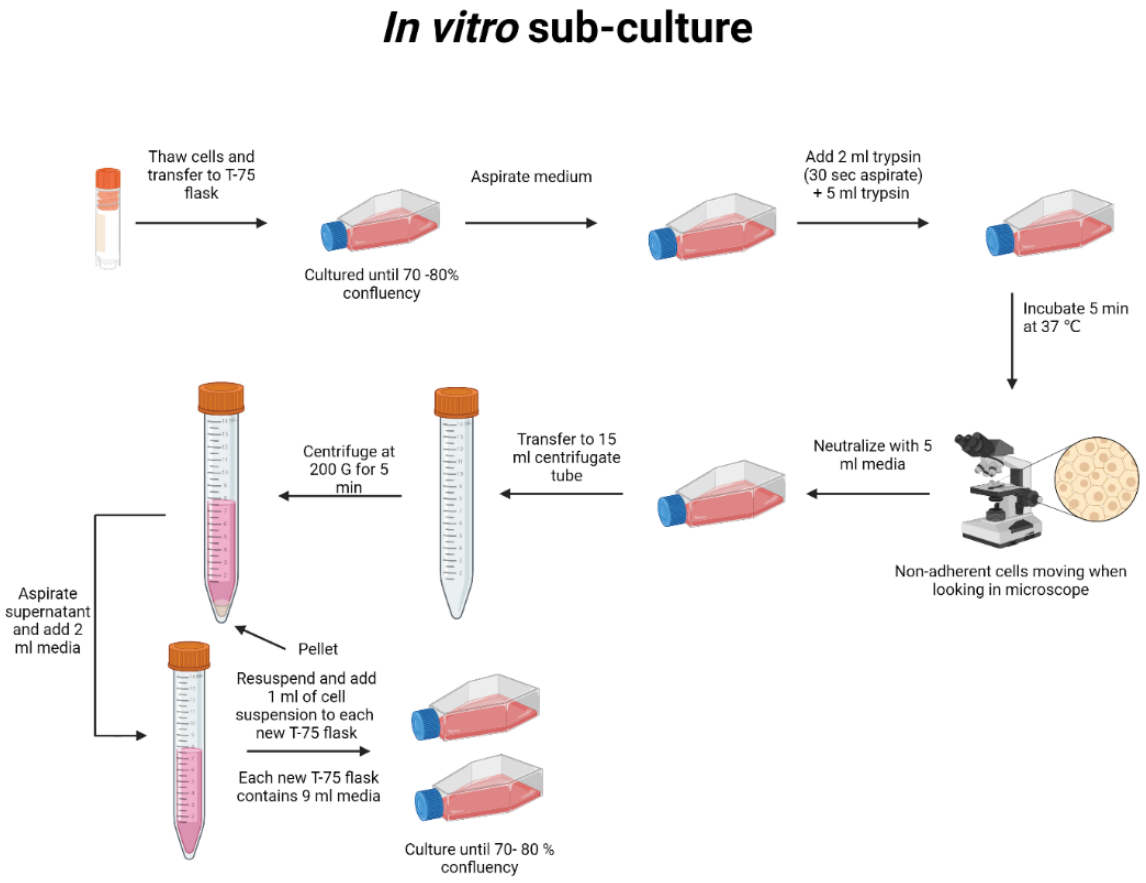

Figure 5. Overview of *in vitro* sub-culture (Created with BioRender.com).

2.5. Preparation of Cadmium Conditioned Media

66 mg Cadmium chloride ($CdCl_2$) (Sigma-Aldrich, #202908) was added to 36 ml of sterile water, and then autoclaved, creating a sterile master mix with 10 mM $CdCl_2$. To create a 10 µM $CdCl_2$ mix, 36 µl from the master mix and 36 ml media were transferred to a 50 ml tube.

To create a 20 µM $CdCl_2$ mix 72 µl from the master mix and 36 ml media were added to a 50 ml tube.

2.6. Proliferation Assay

When the HMVEC-Lymph P7 reached 70% confluency they went through trypsinization and centrifugation (as described earlier). After the supernatant was aspirated, 5 ml of media was added. To count the cells in the cell suspension 10 µl was transferred to a hemocytometer (NanoEnTek, DHC-N01). The cell suspension was calculated to contain 502,000 cells/ml (see Appendix). To get approximately 25,000 cells/well, 0.9 ml of the cell suspension was resuspended and transferred to 35.1 ml of media in a 50 ml tube. Then 2 ml of the new cell suspension was transferred to each well on the three different 6-well plates (VWR), starting with the first well on all plates, before proceeding to the next well. A simplified visual overview of this process is illustrated in Figure 6.

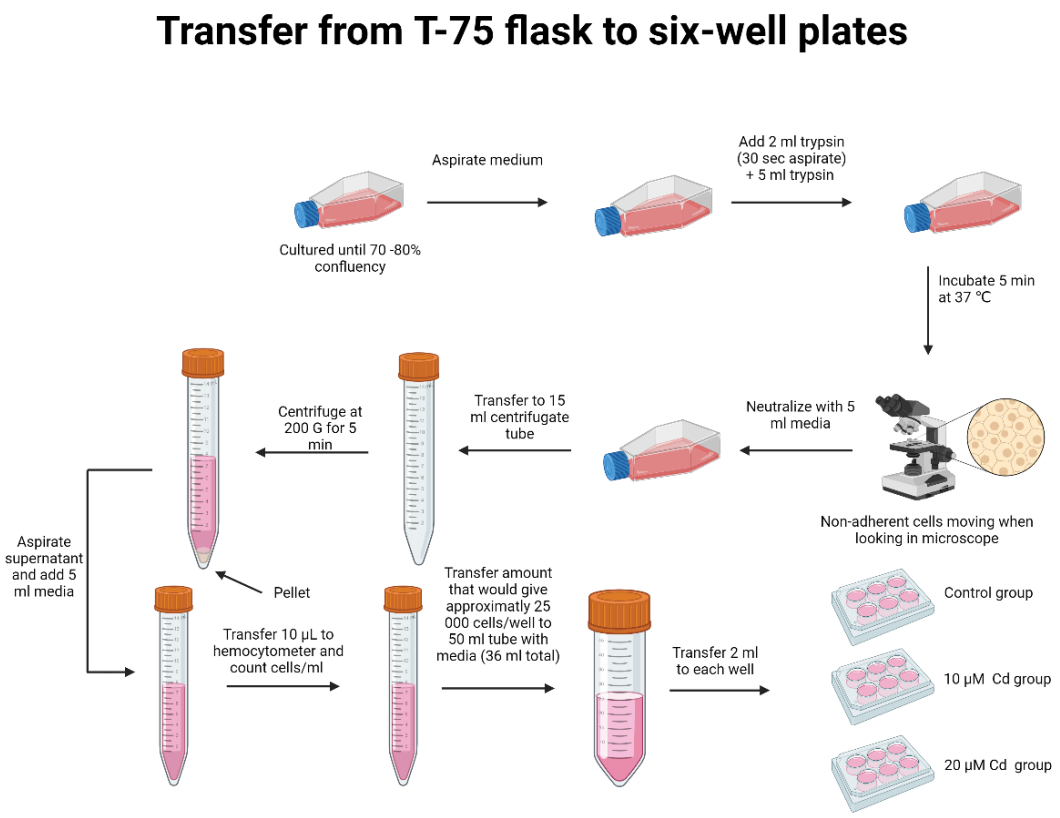

Figure 6. Overview of transfer from T-75 flask to six-well plates (Created with BioRender.com).

After 24 hours 2 ml of 10 µM Cd, 20 µM Cd, and normal media were added to each well of their corresponding group, which starts off day 0 of the HMVEC-dLyAd P8 proliferation assay. The assay continued until day 3, media was changed every 24 hours for each group on days 1 and 2. Cd-media and pipette tips which were in contact with Cd were discarded in a special Cd-container. Pictures were taken for each well at different lens magnifications from day 0 to day 3. On day 3 each well was aspirated, and 0.25 ml of trypsin was added, then incubated for 5 minutes at 37 °C. When the cells detached from the surface of the wells 0.75 ml of media was added. To get an optimal transfer of cells each well was rinsed three times, then transferred to Eppendorf tubes, 6 tubes/plate. The Eppendorf tubes were put on a box of ice. One group at a time, starting with the control group, then 10 µM Cd, and lastly 20 µM Cd, 100 µl of cell suspension from each Eppendorf tube were transferred into a separate 1 ml tube. Additionally, 100 µl of Trypan blue was added to each tube. To count the cell content of each well 10 µl from each tube were resuspended 3 times and transferred to a hemocytometer, and the amount of viable and non-viable cells was counted. A simplified visual overview of this process is illustrated in Figure 7.

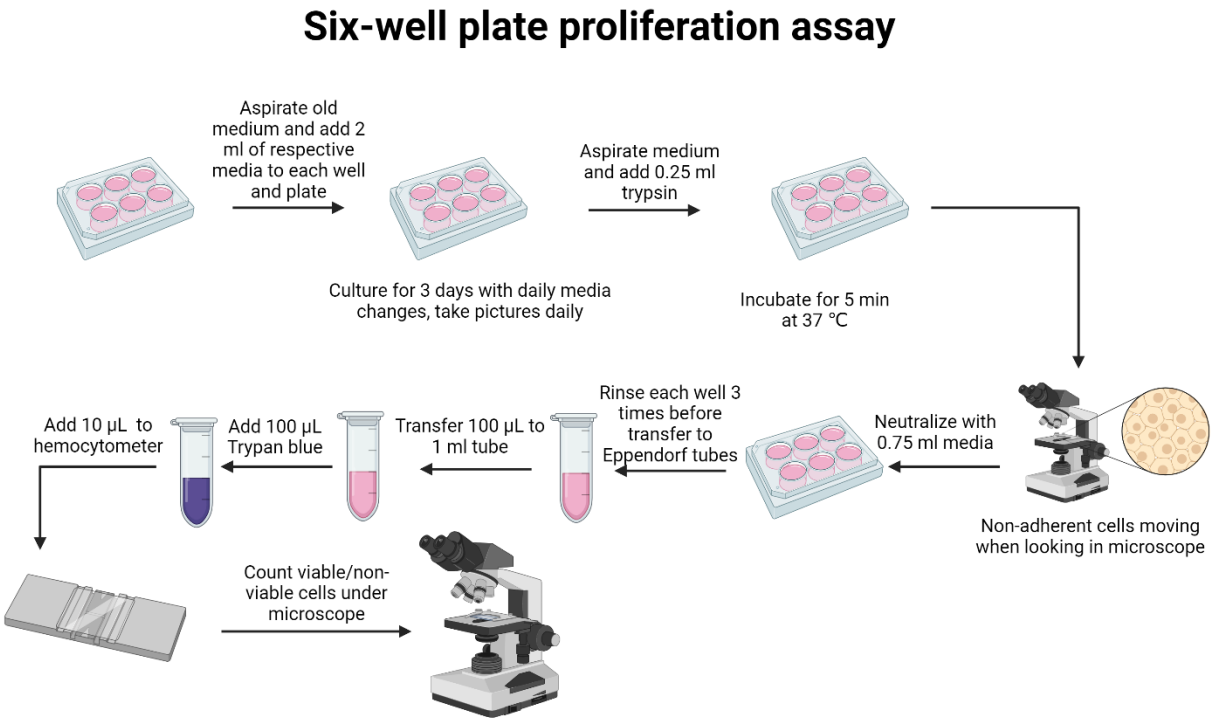

Figure 7. Overview of proliferation assay in six-well plates (Created with BioRender.com).

2.7. Sprouting Assay

2.7.1. Microcarrier Preparation and Cell Incorporation

To prepare the MC suspension 8.4 mg Cytodex 3 microcarriers (Sigma-Aldrich, #GE17-0485-01) were weighed and hydrated with 5 ml non-sterile PBS (Ca^{2+} Mg^{2+} -free, pH 7.4 ± 0.3) (VWR, #392-0442P) in a 15 ml tube for 3 hours. The supernatant was aspirated, and the MCs were washed with new 5 ml of PBS before being autoclaved. Inside the biosafety cabinet supernatant PBS was aspirated, and 4 ml of media at 37 °C was added, then 0.75 ml of cell suspension from HMVEC-dLyAd P7 was transferred to the MC suspension. The HMVEC-dLyAd P8 -microcarrier solution was incubated for 4 hours while tapping/dragging at the bottom of the tube to create a vortex inside to spread the MCs in the solution without getting them stuck on the side of the tube, every 20 minutes. After 4 hours the solution was washed with another 5 ml of media, before being transferred to a T25 flask (VWR). The flask was cultured until 100% confluency on a rotating orbital shaker at 37 °C with 5% CO_2, and 90% humidity, with daily media changes. During daily media changes the MCs were transferred from the T-25 flask into a 15 ml tube, and then the MCs sunk to the bottom before the supernatant fluid was aspirated. Then fresh 5 ml of media was added before being transferred back to the same T-25 flask. A visual overview of this process is illustrated in Figure 8.

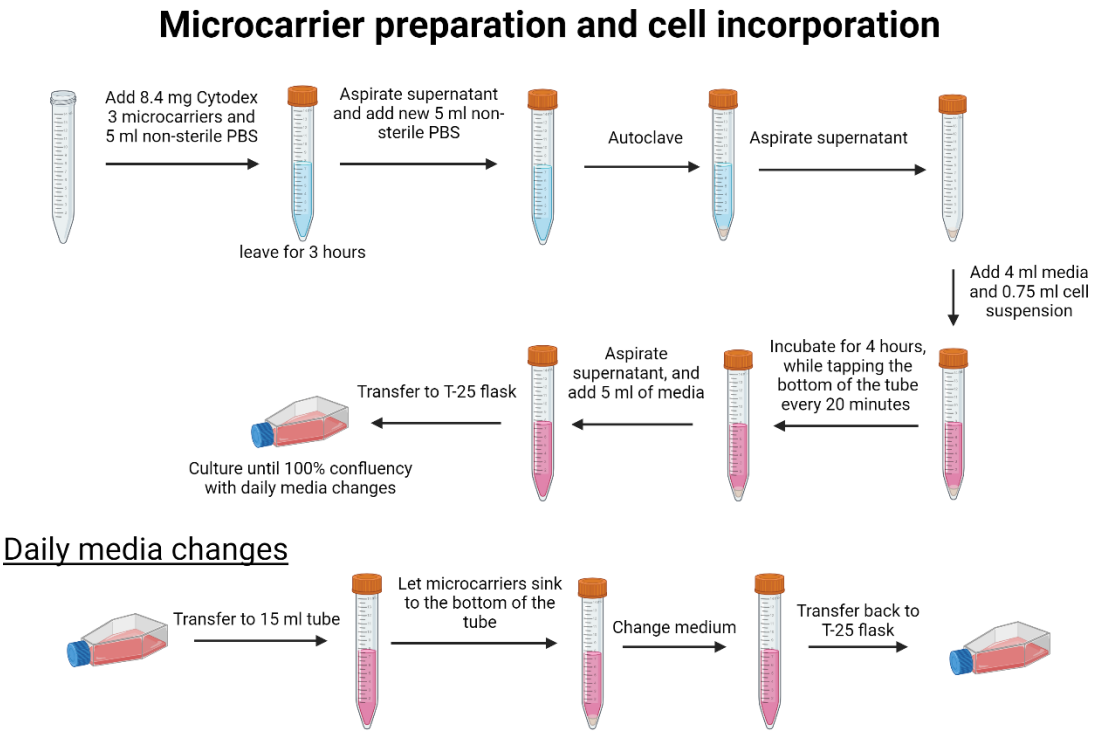

Figure 8. Overview of microcarrier preparation and incorporation of cells (Created with BioRender.com).

2.7.2 Fibrin Gel Preparation

To create the Fibrinogen-solution 50 mg of Fibrinogen (Sigma-Aldrich, #F3879) and 12.5 ml of 0.9 % NaCl were mixed by vortexing and staying in a water bath until it was dissolved. When the Fibrinogen was dissolved it went through a 0.22 μm sterile filter, inside a biosafety cabinet. To create the Thrombin-solution 250 units of Thrombin (Sigma-Aldrich, #T6884) were dissolved in 10 ml of PBS. To create the Aprotinin-solution 5 mg of Aprotinin (Sigma-Aldrich, #A4529) was dissolved in 10 ml of PBS. Solution A was made by adding 3.3 ml of PBS and 0.3 ml of the thrombin solution. Solution B was made by adding 3 ml of the fibrinogen solution, 0.4 ml of the Aprotinin solution, and 1 ml of microcarrier-HMVEC-dLyAd P8 solution.

Solution B (0.25 ml) was added to each well of the first two columns, and three wells on the last two columns on a 24-well plate (VWR) (14 wells total). Excess bubbles and foam left in Solution B prevented the gel formation in the final two wells. Additionally, 0.20 ml of Solution A was added to each well with Solution B and resuspended three times, if bubbles were created, they were removed. After one row was finished the plate was moved in a figure-eight motion to distribute the gel around and cover the well, until Solution A had been added to every well with Solution B. This process was repeated to create one more plate but on the next day. The gels were left to rest for 1 hour in the incubator before adding media. To the first column of both plates, 0.8 ml regular media was added. 10 μM Cd-media was added to the last 10 wells of the first plate, and 20 μM Cd-media was added to the last 10 wells on the other plate, starting day 0 of the HMVEC-dLyAd P9 sprouting assay. After 24 hours new 0.8 ml of respective media was added to each well on both plates. Daily media changes occurred until day 4, Cd-media was disposed of in respective containers. Pictures were taken at 10x and 20x magnitudes for each day. On day 4 media was aspirated and 0.8 ml sterile PBS was added to each well. Then the PBS was aspirated, and 8 ml formalin (4 %) was added to each well inside the fume hood and stored in the fridge at 4 ℃ overnight. The formalin was aspirated, and 0.8 ml non-sterile PBS was added to each well to keep the gels hydrated. Then MCs and sprouts were manually counted for each well using the microscope. A visual overview of this process is illustrated in Figure 9.

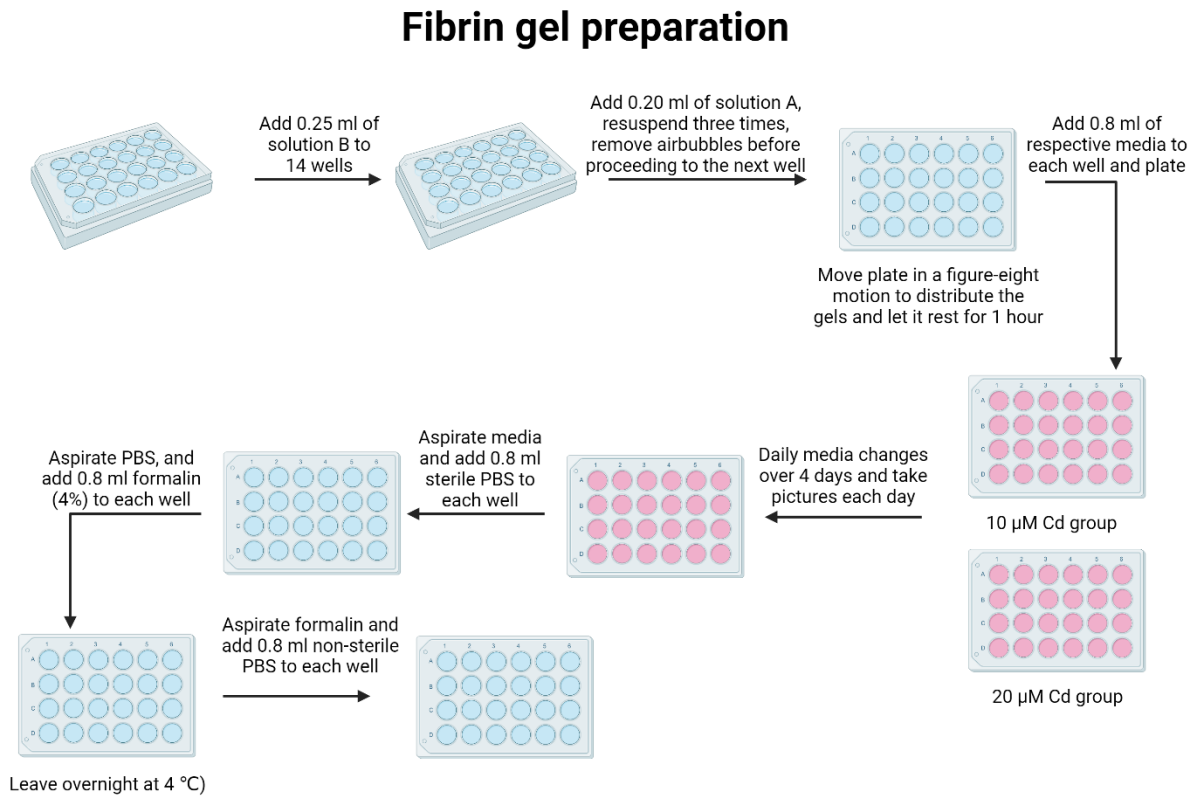

Figure 9. Overview of Fibrin gel preparation (Created with BioRender.com).

3. Results

3.1. Proliferation Assay

To examine how Cd impacted proliferation and cell viability, proliferation assays with a control group and different concentrations of Cd (10 and 20 µM) were conducted over 3 days. Upon examining the microscopy pictures of the proliferation assays in Figure 10, Figure 11, and Figure 12, we observe that the cells have become more confluent and look healthy.

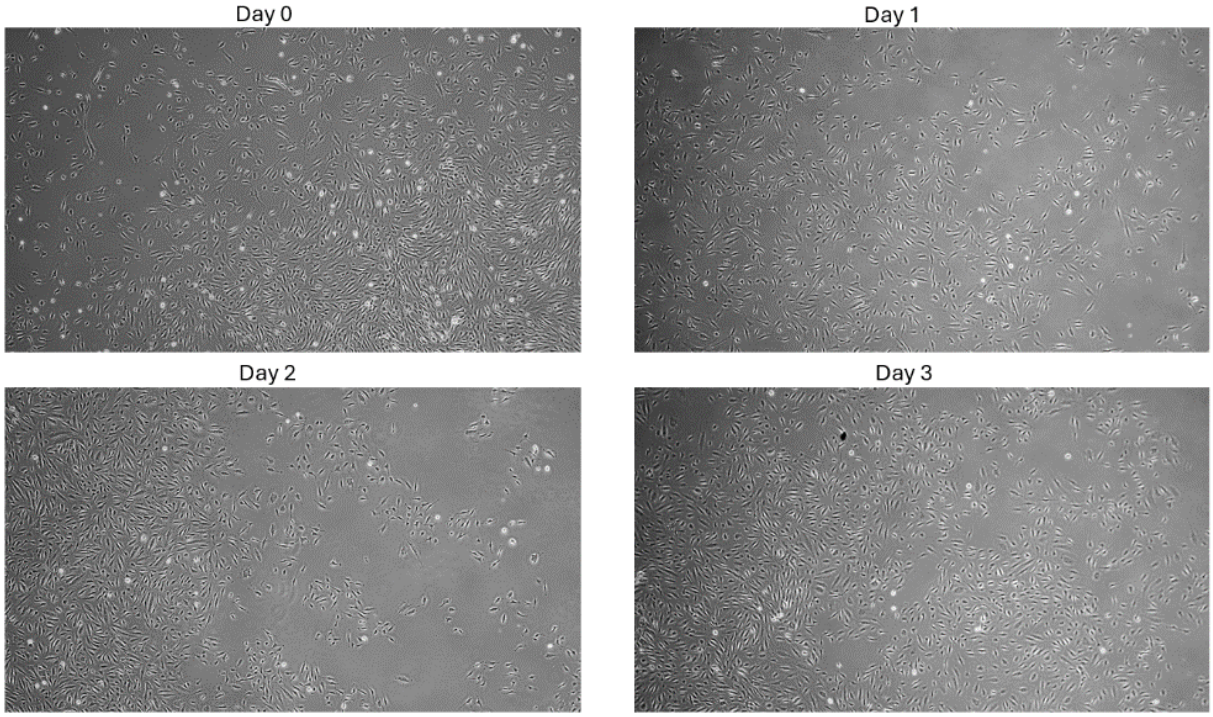

Figure 10. Control group proliferation assay HMVEC-dLyAd P8, all pictures were taken from the same well with 4x lens magnification.

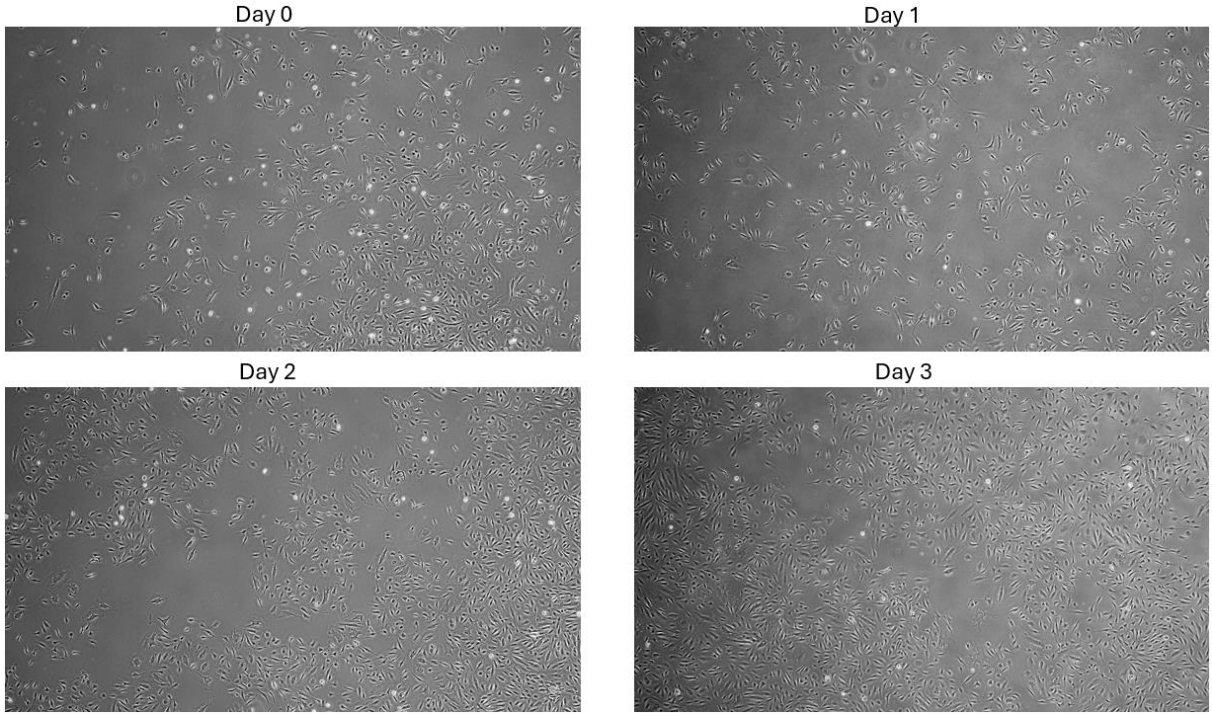

Figure 11. 10 µM Cd group proliferation assay HMVEC-dLyAd P8, all pictures were taken from the same well with 4x lens magnification.

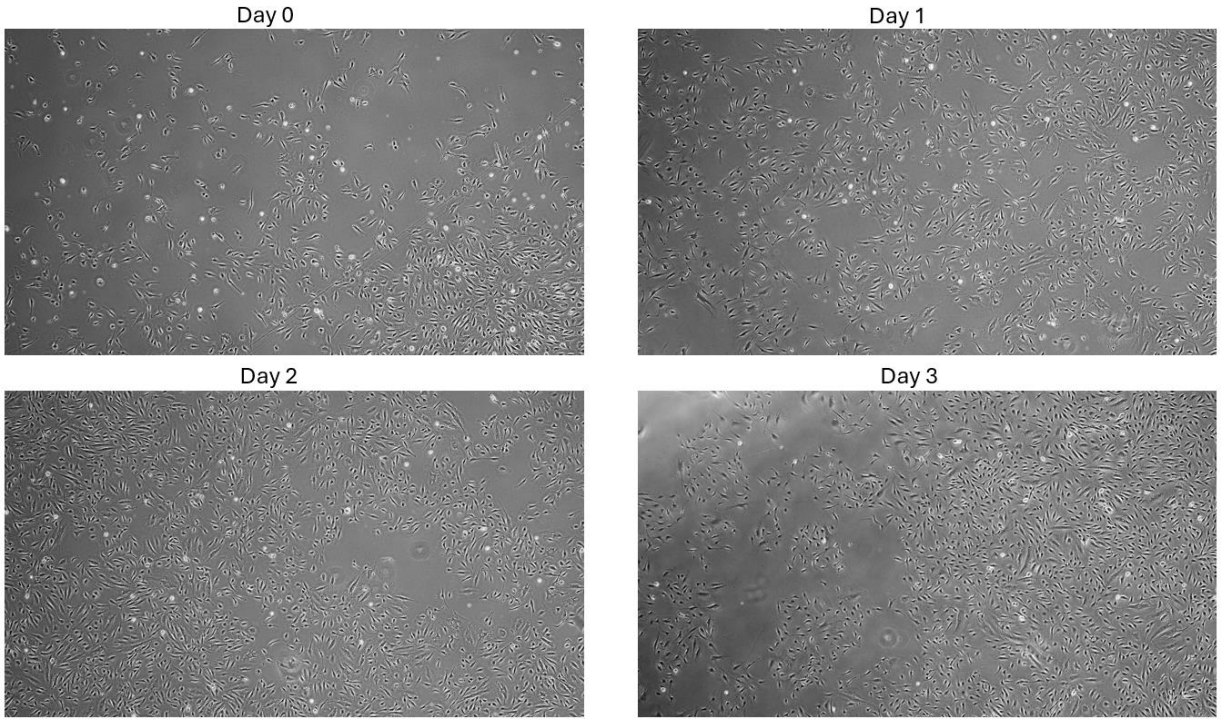

Figure 12. 20 µM Cd group proliferation assay HMVEC-dLyAd P8, all pictures were taken from the same well with 4x lens magnification.

When reviewing the images in Figure 10, Figure 11, and Figure 12 the cells exposed to cadmium look healthy. However, cell counting with Trypan blue staining revealed that there were significantly fewer viable cells than first thought. Analysing the data collected from the cell count, as depicted in Figure 13, we can observe the number of viable cells in the cadmium-exposed groups is significantly lower compared to the control group. Additionally, Figure 14 depicts a substantially higher proportion of non-viable cells in the Cd-exposed groups than in the control group. The control group exhibited a viability rate of 63.01 %. In contrast, the 10 µM Cd group only maintained a viability rate of 23.76 %, and the 20 µM Cd group had an even lower rate at 22.75 % (calculations in Appendix).

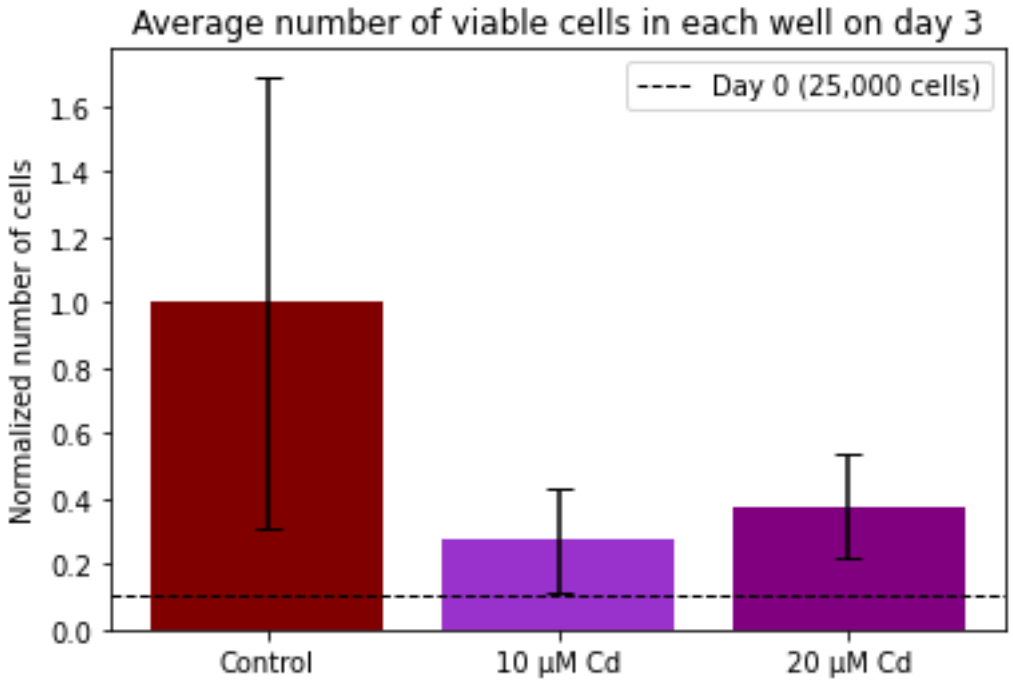

Figure 13. Graphical analysis of viable cells from proliferation assay.

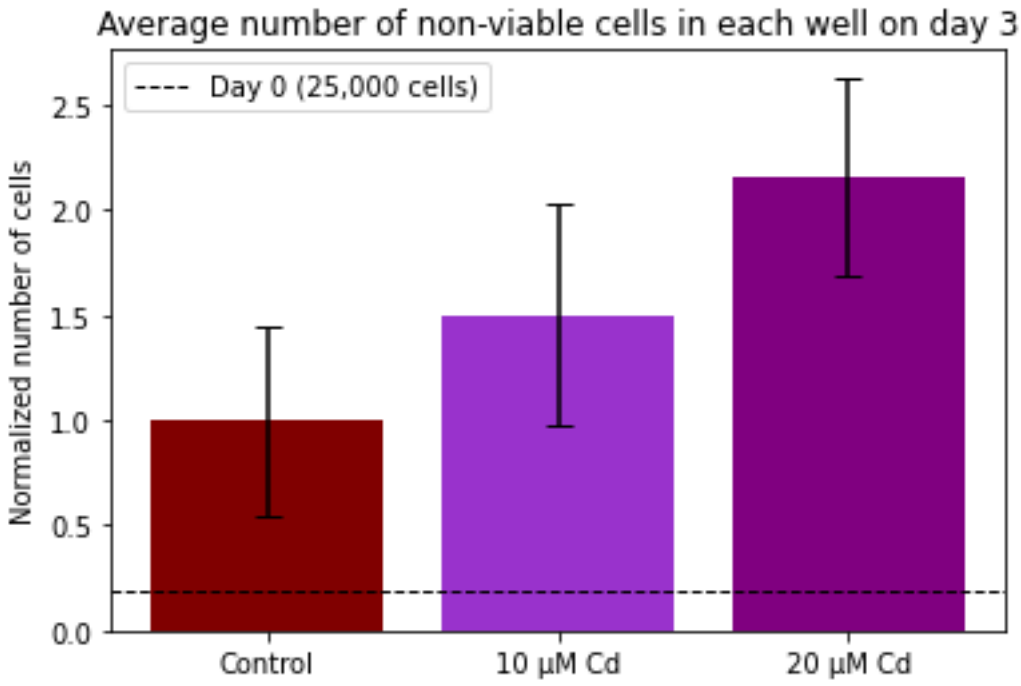

Figure 14. Graphical analysis over non-viable cells from proliferation assay.

As depicted in Figure 13 and Figure 14 there are overall fewer cells in the 10 µM group compared to the two other groups suggesting a non-uniform transfer of cells to each well of the proliferation assays. Figure 15 also illustrates that there are significantly fewer cells in one of the wells of the 10 µM Cd group. By examining Figure 15 significantly less proliferation is observed compared to the previously shown figures.

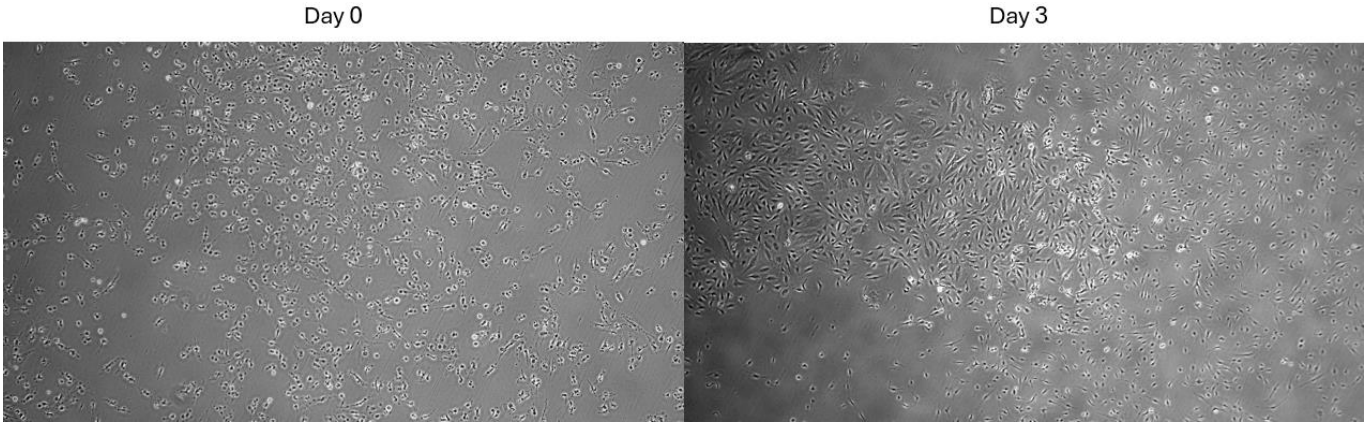

Figure 15. 10 µM Cd group proliferation assay HMVEC-dLyAd P8, both pictures were taken from well no. 4 with 4x lens magnification.

3.2. Sprouting Assay

To assess the effect Cd had on the sprouting of HMVEC-dLyAd P9, a 3D sprouting assay which mimics early events of lymphangiogenesis was conducted over 4 days, and the cells were exposed to different concentrations of Cd (10 and 20 µM) (70). A sprout was defined as an elongated structure extending from the MC consisting of a minimum of 2 endothelial cells, resulting in a length approximately half the radius of the microcarrier for reference. Examining the pictures in Figure 16 it was observed that the control group exhibited significant sprouting over 4 days.

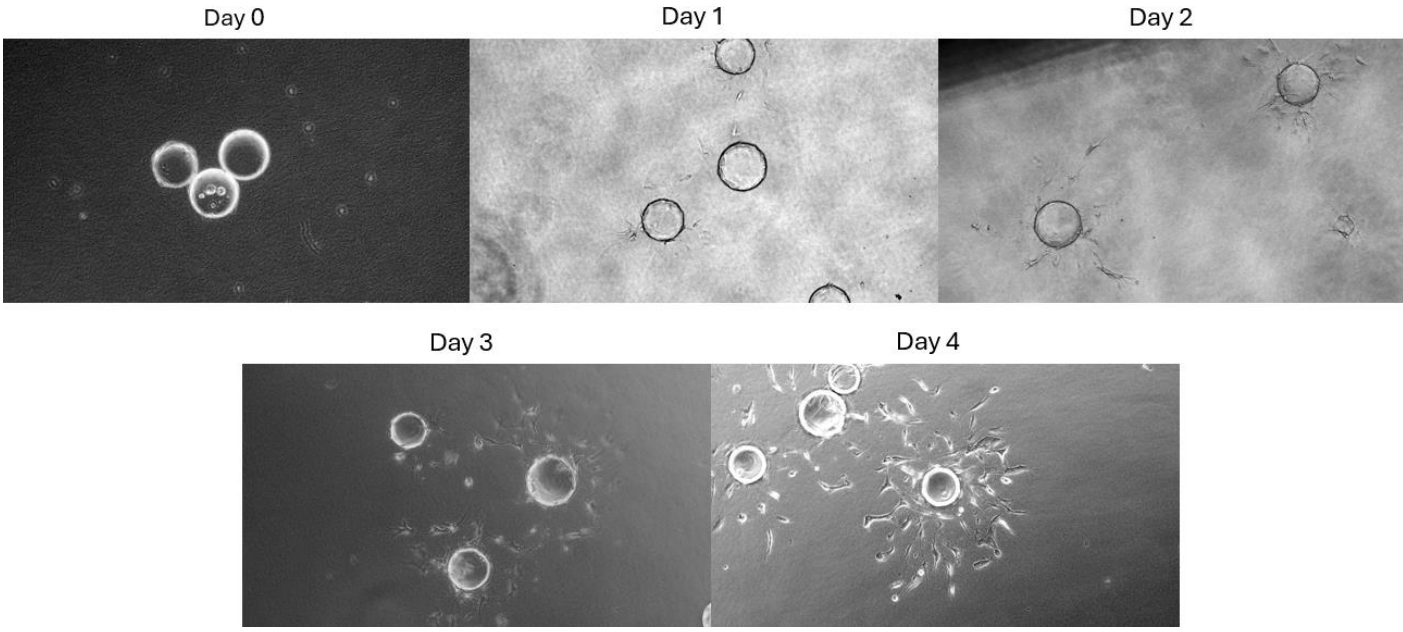

Figure 16. Control group sprouting assay HMVEC-dLyAd P9, all pictures were taken from random wells with 10x lens magnification.

The 10 µM Cd group had significant proliferation around the MCs but did not exhibit any sprouting as illustrated in Figure 17. On day 1 in Figure *17* it is observable that certain cells have detached from the microcarriers. These HMVEC-dLyAd P9 cells proliferated around the MCs like a barrier throughout this assay. Figure 18 is a higher magnification of day 4 on Figure 17, and depicts a highly confluent area of proliferated HMVEC-dLyAd P9 cells.

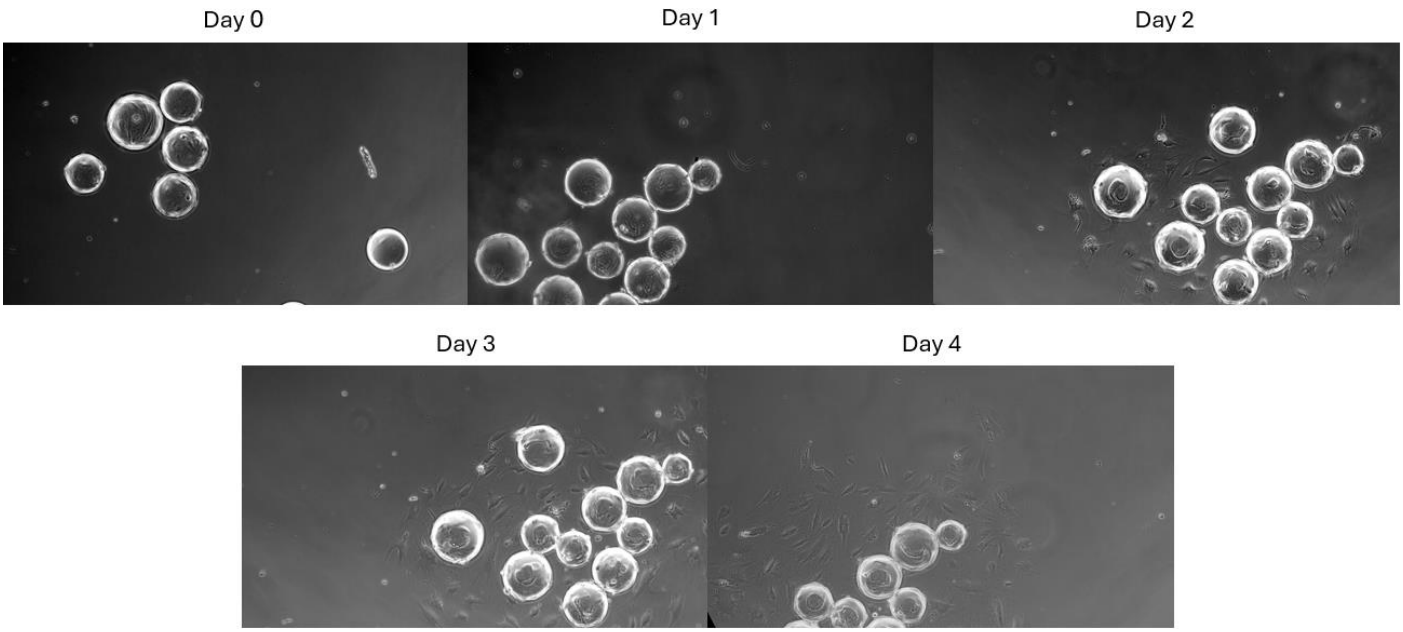

Figure 17. 10 µM Cd group sprouting assay HMVEC-dLyAd P9, all pictures were taken from the same well with 10x lens magnification.

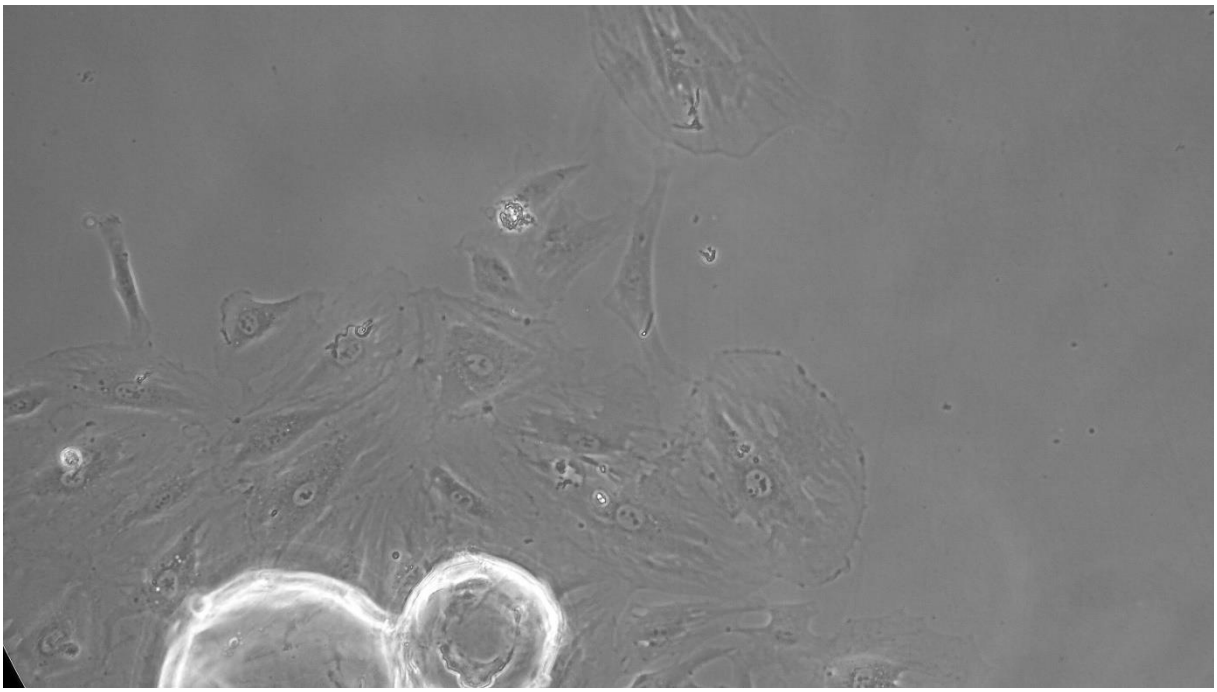

Figure 18. 10 µM Cd group sprouting assay HMVEC-dLyAd P8, the picture is taken at the same location as day 4 in Figure 17 with 20x lens magnification.

By comparing Figure 16, Figure 17 and Figure 19 there are visibly significantly fewer cells in the 20 µM Cd group compared to the control group and 10 µM, however, there were still some sprouts on day 4 of the sprouting assay.

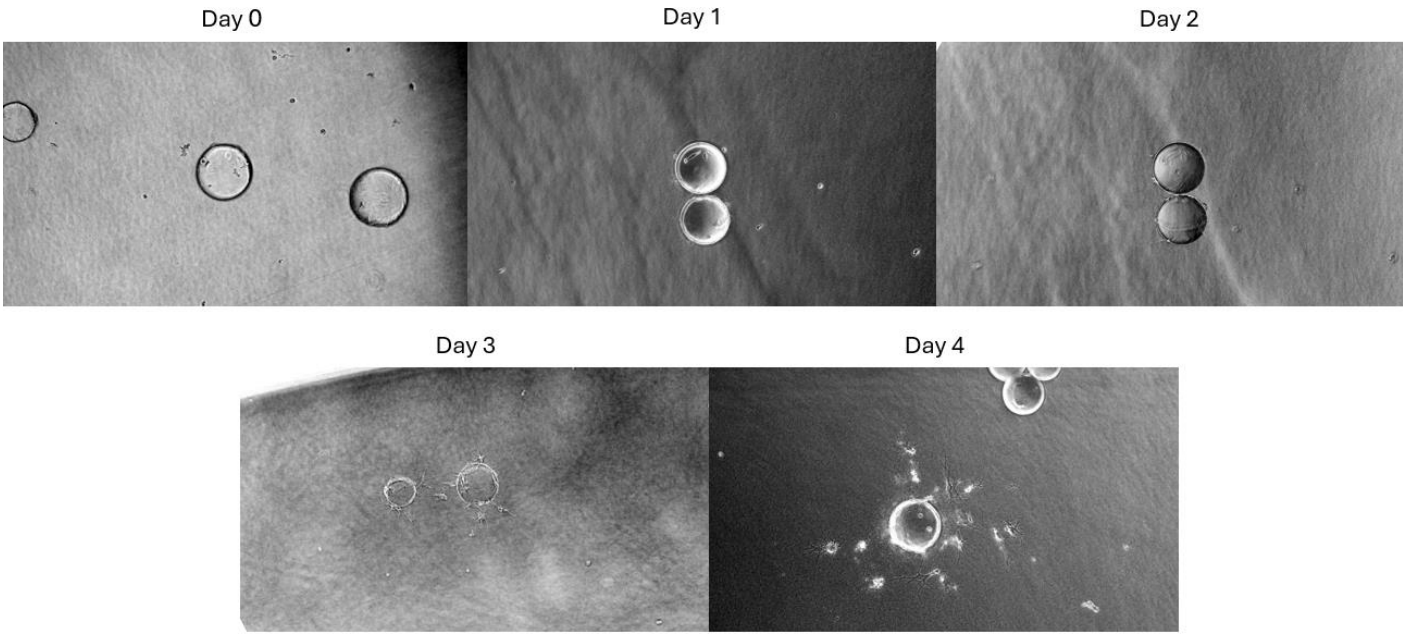

Figure 19. 20 µM Cd group sprouting assay HMVEC-dLyAd P8, all pictures were taken from the same well at different locations with 10x lens magnification.

The control group had the most sprouts/MC with an average of 1.89, the 10 µM Cd group had 0 sprouts/MC, and the 20 µM group had an average of 0.67 sprouts/MC as observed in Figure 20. Additionally, the sprouts from the control group appear to be longer than the ones in the 20 µM group when comparing Figure *16* and Figure *19*.

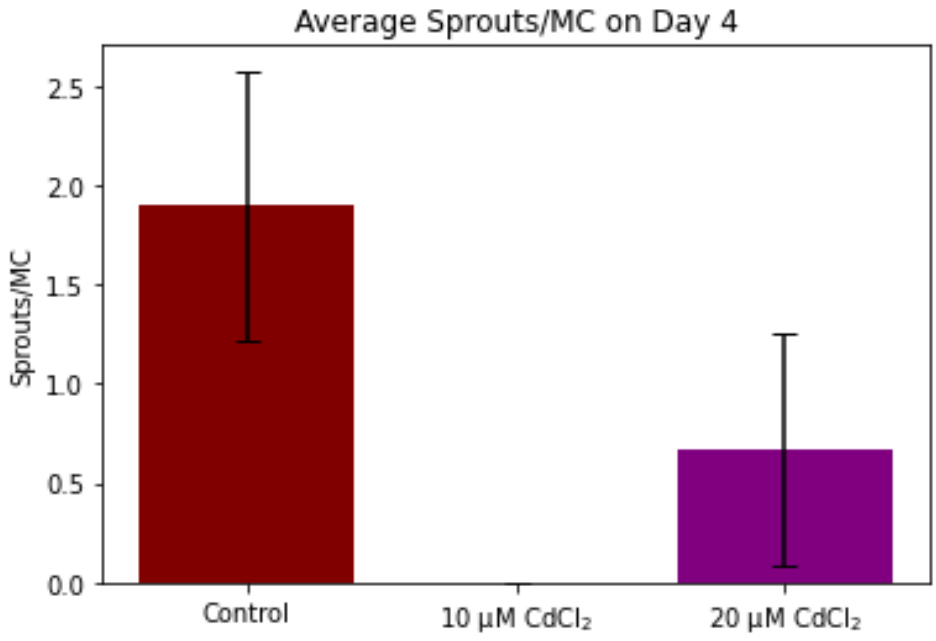

Figure 20. Graphical analysis of Sprouts per MC in different concentrations of Cd.

In the majority of the wells, there were numerous clustered MCs, this resulted in less available sprouting area for cells adhered to the MCs. This phenomenon is depicted in Figure 21.

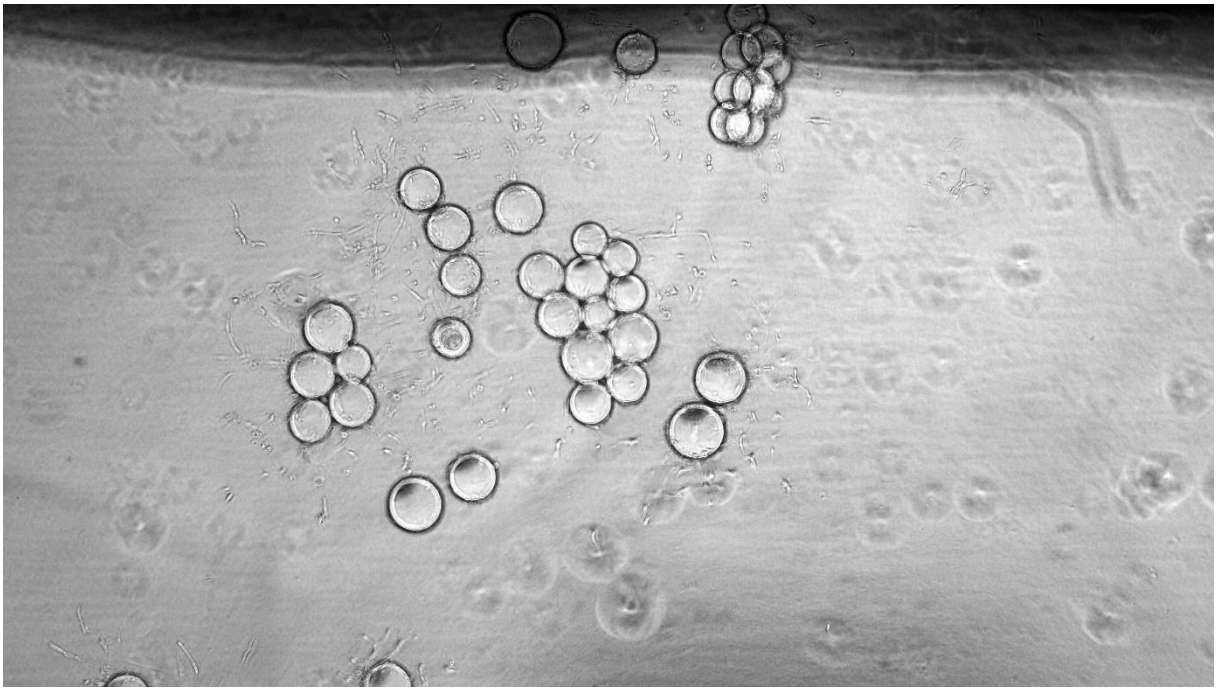

Figure 21. Control group sprouting assay HMVEC-dLyAd P9 day 4, depicting clustered microcarriers, the picture was taken with 4x lens magnitude.

4. Discussion

4.1. Proliferation Assay

The results of the proliferation assay suggest that Cd has a substantial impact on proliferation and cell viability in the HMVEC-dLyAd P8 cultures. As depicted in Figure 13 the cell viability of the Cd groups had a drastic decrease compared to the control group. All the groups became more confluent over the three-day duration of the proliferation assay suggesting that the Cd concentrations were not sufficient to fully inhibit proliferation, but enough to drastically reduce cell viability. Additionally, there were a lot more non-viable cells which were not adherent in the Cd groups, especially in the 20 µM group. However, these cells were aspirated before cell counting and the cell viability was only determined by the adherent cells which looked healthy. This phenomenon could be explained by an accumulation of Cd throughout the proliferation assay. During the proliferation assay daily media changes were performed, adding in new Cd-conditioned media, potentially leading to accumulation and overall higher concentrations.

There are several studies suggesting that Cd can accumulate in cells, stop proliferation, and cause cell death when concentrations are high enough (77). Prior studies on how Cd affect the proliferation of HMVEC and HUVEC contradict the results obtained in this thesis. One study did not observe a decrease in cell viability after treatment with concentrations of 1 µM up to 1mM Cd, 50 times higher than 20 µM, but they were only treated for 6 and 18 hours (3). During the conducted proliferation assay, a concentration of 60 µM is the highest possible concentration that could be obtained through accumulation in the 20 µM Cd group.

There is minimal difference between the cell viability of the 10 µM and 20 µM groups. The data from the cell viability plot are not 100 % accurate as there was a non-uniform distribution of cells to each well. This was observable in the microscope, especially in the 10 µM group there were significantly fewer cells in some of the wells as depicted in Figure 15. This would result in a higher Cd concentration per cell in those wells than the 20 µM group (Calculations in Appendix), which could explain the low cell viability as they had significantly less proliferation as depicted in Figure 15.

These discoveries could suggest that HMVEC-dLyAd is more sensitive to the cytotoxic effects of Cd compared to HMVEC and HUVEC. However, this thesis and the prior study utilized different treatment durations, suggesting duration of treatment also affects cell viability. Additionally, the results suggest that the dose-response relationship is affected by the cell density of the treated culture.

Potential errors that might have occurred during this proliferation assay would be inconsistent pipetting due to a non-uniform distribution of cells from the cell suspension to the six-well plates. The disadvantage of using a hemocytometer for cell counting is that humans can make errors while mixing, diluting, and pipetting. When using a hemocytometer there is also a need for multiple cell sample counts to ensure statistical accuracy, which was not conducted as there were limited resources, there is also a non-uniform distribution of cells in the observation area (78). In some of the samples, cells were clustered together making it hard to get an accurate count as estimations were required to determine approximately how many cells were in these clusters.

4.2. Sprouting Assay

The results of the sprouting assay suggest that Cd had a substantial impact on HMVEC-dLyAd P9 sprouting. Sprouting was observed in the 20 µM group however, it was less than in the control group as depicted in Figure 20. The 10 µM group showed no sprouting at all,

however they seemed to have started to proliferate around the MCs. Figure 17 depicts that the MCs are covered in cells, this suggests that they somehow have detached and started to proliferate in the gel rather than sprouting from the MCs. This was most likely not induced by Cd as the 20 µM group did have some sprouts, but no proliferation around the MCs. Katayama et al. showed that mechanical forces such as pipetting can cause basal cells to detach from Cytodex 3 MCs (79). By analysing day 1 in Figure 17, there are certain LECs detached, while other LECs are still attached to the MCs. This suggests that vigorous pipetting may have occurred, resulting in the detachment of cells from MCs. The detached cells proliferated around the MCs, suggesting they did not differentiate into tip and stalk cells forming sprouts. These cells occupied the sprouting area like a barrier and may have physically inhibited the LECs still attached to the MCs from sprouting.

The control group had significantly more sprouts than the 20 µM Cd group, and they were longer, suggesting that this concentration of Cd did not inhibit sprouting completely, but negatively affected the sprouting of HMVEC-dLyAd P9.

The sprouting assays were performed on different days due to unforeseen circumstances. The 10 and 20 µM assays with control groups conducted on April 12th were compromised. The 10 µM assay was conducted on April 13th, and unforeseen resource and equipment limitations prohibited the 20 µM group from being performed until April 14th. On April 15th EGM™-2MV Medium was depleted, compromising the control groups in the 10 and 20 µM assays. Another researcher from the Silva research group conducted the same sprouting assay with only a control group on April 12th and performed media change on April 15th. Permission to use the control group was granted. The MCs in the different sprouting assays were retrieved from the same suspension, however as depicted in Table 4, Table 5, and Table 6 (see appendix) it was observed a significant decrease in MCs in the Cd groups. This discrepancy may be explained by the sequential transfer of MC suspension. As the control group were prepared first, MCs could have accumulated in the corner of the T-25 flask, resulting in the transfer of a higher concentration of MC suspension. This would lower the concentration of MC suspension for the subsequent Cd groups.

The control group had a lot of clustered MCs, denying a lot of sprouting area resulting in a lower number of sprouts per MC. The number of MCs coated with cells was also not counted, giving an inaccurate measurement of sprouts per MC as there can be no sprouting if the MCs are not coated. These are factors that affect the reliability of this experiment.

5. Conclusion

This thesis is a first step in trying to understand the complicated impact of how Cd affects lymphangiogenesis. The results should be looked at critically as there are some reliability issues, however other studies on endothelial cells like HUVEC and HMVEC-d claim that Cd is cytotoxic and negatively impacts cell viability, proliferation, sprouting and tube formation at high enough concentrations (3). The results of this thesis suggest that concentrations of 10 and 20 µM Cd are not sufficient to completely inhibit proliferation and sprouting, but significantly decrease cell viability. Prior studies did not observe reduced cell viability even at 1 mM Cd, 50 times higher than 20 µM. The significant decrease in cell viability could suggest that HMVEC-dLyAd is more sensitive to Cd than HUVECs and HMVECs, however further research is necessary before any conclusions can be made. The results acquired in this thesis suggest that Cd possibly could cause lymphatic dysfunction and lead to lymphedema (48). Authorities worldwide must take every measure to reduce Cd emissions and remove Cd from soil and water with remediation techniques. Additionally, consumers should avoid Cd-rich foods and products as their accumulation may lead to adverse health implications over time. Overall, the findings in this thesis are an important starting point for understanding how Cd affects LEC proliferation and sprouting. Further research is needed to reveal the mechanisms of this complicated topic.

6. Future Directions

The findings in this thesis are important starting points for understanding how Cd affects LEC proliferation and sprouting, however further research is necessary to acquire a broader and deeper understanding. It could be beneficial to replicate the experiments conducted in this thesis to gather more data and exclude certain errors that occurred. For both the proliferation and sprouting assays, measures must be implemented to ensure a uniform distribution of cells and MCs to achieve consistent and reliable results. Consistency in sprouting assay preparation should be prioritized, and all assays conducted at the same time to minimize batch effects that could influence the results. Using flow cytometry or an automated fluorescence microscopic cell counter to count cells from the proliferation assay instead of a hemocytometer with Trypan blue staining could be beneficial. It would exclude human errors and provide a more reliable and accurate count (80). For both assays, a wider range of Cd concentrations could be advantageous as it would provide a better understanding of the dose-response relationship.

For the proliferation assay, the cells should counted at several different time points, to investigate the effects of treatment duration. It would be interesting to analyse the gene expression of VEGFR-3 in the sprouting assay, as it is prominently expressed on the tip cells of sprouting lymphatic vessels (55). Additionally, it would be exciting to investigate how Cd impacts LEC tube formation as this thesis only looked at proliferation and sprouting.

7. References

1. Chunhabundit R. Cadmium Exposure and Potential Health Risk from Foods in Contaminated Area, Thailand. Toxicol Res. 2016;32(1):65-72.
2. Padera TP, Meijer EF, Munn LL. The Lymphatic System in Disease Processes and Cancer Progression. Annu Rev Biomed Eng. 2016;18:125-58.
3. Woods JM, Leone M, Klosowska K, Lamar PC, Shaknovsky TJ, Prozialeck WC. Direct antiangiogenic actions of cadmium on human vascular endothelial cells. Toxicol In Vitro. 2008;22(3):643-51.
4. Tchounwou PB, Yedjou CG, Patlolla AK, Sutton DJ. Heavy metal toxicity and the environment. Exp Suppl. 2012;101:133-64.
5. Fjellvåg H. tungmetaller: Store Norske Leksikon; 2020 [Available from: https://snl.no/tungmetaller.
6. Singh R, Gautam N, Mishra A, Gupta R. Heavy metals and living systems: An overview. Indian J Pharmacol. 2011;43(3):246-53.
7. Briffa J, Sinagra E, Blundell R. Heavy metal pollution in the environment and their toxicological effects on humans. Heliyon. 2020;6(9):e04691.
8. Jadav S. EFFECTS OF HEAVY METAL TOXICITY FROM FISH TO HUMANS. 2022. p. 54-60. Figure 3, Release of industrial wastes increase the concentration of heavy metals (Pb, As, Hg,

Cd) in aquatic system; p. 58.
9. Jaishankar M, Tseten T, Anbalagan N, Mathew BB, Beeregowda KN. Toxicity, mechanism and health effects of some heavy metals. Interdiscip Toxicol. 2014;7(2):60-72.
10. Grandjean P, Bellanger M. Calculation of the disease burden associated with environmental chemical exposures: application of toxicological information in health economic estimation. Environmental Health. 2017;16(1):123.
11. European Environment Agency. Heavy metal emissions in Europe: EEA; 2023 [Available from: https://www.eea.europa.eu/en/analysis/indicators/heavy-metal-emissions-in-europe?activeAccordion=.
12. Gaur VK, Sharma P, Gaur P, Varjani S, Ngo HH, Guo W, et al. Sustainable mitigation of heavy metals from effluents: Toxicity and fate with recent technological advancements. Bioengineered. 2021;12(1):7297-313.
13. Agency for Toxic Substances and Disease Registry. ATSDR's Substance Priority List: ATSDR; 2023 [Available from: https://www.atsdr.cdc.gov/spl/index.html#2022spl.
14. National Center for Biotechnology Information. PubChem Element Summary for AtomicNumber 48, Cadmium: PubChem; 2024 [Available from: https://pubchem.ncbi.nlm.nih.gov/element/Cadmium.
15. Faroon O, Ashizawa A, Wright S, Tucker P, Jenkins K, Ingerman L, Rudisill C. RELEVANCE TO PUBLIC HEALTH. 2012. In: Toxicological Profile for Cadmium [Internet]. Atlanta: Agency for Toxic Substances and Disease Registry. Available from: https://www.ncbi.nlm.nih.gov/books/NBK158837/.
16. Kubier A, Wilkin RT, Pichler T. Cadmium in soils and groundwater: A review. Appl Geochem. 2019;108:1-16.

17. Tang L-l, Fu B-m, Wu Y, Cai F-c, Ma Y-b. Linking atmospheric emission and deposition to accumulation of soil cadmium in the Middle-Lower Yangtze Plain, China. Journal of Integrative Agriculture. 2023;22(10):3170-81.
18. Shacklette HT. Cadmium in Plants1972 28.02.2024. Available from: https://pubs.usgs.gov/bul/1314g/report.pdf.
19. Health Protection Agency. Cadmium

Toxicological overview: HPA; 2010 [Available from: https://assets.publishing.service.gov.uk/media/5a7dbec6e5274a5eb14e6ee1/hpa_cadmium_toxicological_overview_v3.pdf.
20. Asagba SO. Cadmium Absorption. In: Kretsinger RH, Uversky VN, Permyakov EA, editors. Encyclopedia of Metalloproteins. New York, NY: Springer New York; 2013. p. 332-7.
21. Dartmouth Toxic Metals. The Facts on Cadmium 2022 [Available from: https://sites.dartmouth.edu/toxmetal/more-metals/cadmium-an-illusive-presence/the-facts-on-cadmium/.
22. Department of Public Health EaSDoH. World Health Organization; 2019 [Available from: https://iris.who.int/bitstream/handle/10665/329480/WHO-CED-PHE-EPE-19.4.3-eng.pdf.
23. Agency for Toxic Substances and Disease Registry. Who Is at Risk of Cadmium Exposure? : ATSDR; 2023 [Available from: https://www.atsdr.cdc.gov/csem/cadmium/Who-Is-at-Risk.html.
24. World Health Organization. Tobacco: WHO; 2023 [Available from: https://www.who.int/news-room/fact-sheets/detail/tobacco.
25. Worldometer. Current World Population: Worldometers.info; 2024 [Available from: https://www.worldometers.info/world-population/.
26. Norwegian Scientific Committee for Food Safety. Risk assessment of dietary cadmium exposure in the Norwegian population: VKM; 2015 [Available from: https://vkm.no/download/18.2994e95b15cc54507161525b/1498142416154/07cfa5d365.pdf
27. Miljødirektoratet. Kadmium og kadmiumforbindelser: Miljødirektoratet; 2023 [Available from: https://miljostatus.miljodirektoratet.no/tema/miljogifter/prioriterte-miljogifter/kadmium-og-kadmiumforbindelser/.
28. FHI. Kadmium i mat og miljø: Folke Helse Instituttet; 2022 [Available from: https://www.fhi.no/kl/miljogifter/fakta/kadmium-i-mat-og-miljo--faktaark/#inntak-av-kadmium-i-norge-og-europa.
29. Norwegian Scientific Committee for Food Safety. Risk assessment of dietary cadmium exposure in the Norwegian population: VKM; 2015. Figure 3.1-1, Mean concentrations of cadmium (Cd) in Norwegian food and food groups; p. 45 [Available from: https://vkm.no/download/18.2994e95b15cc54507161525b/1498142416154/07cfa5d365.pdf
30. Mattilsynet. Kadmium: Mattilsynet; 2023 [Available from: https://www.mattilsynet.no/mat-og-drikke/uonskede-stoffer-i-mat/miljogifter/ulike-typar-miljogifter/kadmium.
31. Rafati Rahimzadeh M, Rafati Rahimzadeh M, Kazemi S, Moghadamnia AA. Cadmium toxicity and treatment: An update. Caspian J Intern Med. 2017;8(3):135-45.
32. Ozra M. Itai Itai Disorder: Causes, Symptoms, and Treatment: Journal of Heavy Metal Toxicity and Diseases; 2023 [Available from: https://www.primescholars.com/articles/itai-itai-disorder-causes-symptoms-and-treatment-124269.html.
33. Mehdikhanmahaleh MM, Tabatabaei-Malazy O. Itai itai disease: Elsevier; 2023 [Available from: https://www.sciencedirect.com/topics/pharmacology-toxicology-and-pharmaceutical-science/itai-itai-disease.
34. Dökmeci A, Ongen A, Dagdeviren. Environmental Toxicity of Cadmium and Health Effect. Journal of environmental protection and ecology. 2009;10:84-93. Figure 3, Itai-itai disease and bone structure; p. 88.
35. Cleveland Clinic. Atherosclerosis: Cleveland Clinic; 2024 [Available from: https://my.clevelandclinic.org/health/diseases/16753-atherosclerosis-arterial-disease.

36. Messner B, Knoflach M, Seubert A, Ritsch A, Pfaller K, Henderson B, et al. Cadmium is a novel and independent risk factor for early atherosclerosis mechanisms and in vivo relevance. Arterioscler Thromb Vasc Biol. 2009;29(9):1392-8.
37. Wätjen W, Beyersmann D. Cadmium-induced apoptosis in C6 glioma cells: influence of oxidative stress. Biometals. 2004;17(1):65-78.
38. Ozdowski L, Gupta V, editors. Physiology, Lymphatic System. Treasure Island (FL): StatPearls Publishing; 2023.
39. The Editors of Encyclopaedia Britannica. lymphatic system: Encyclopedia Britannica; 2024 [Available from: https://www.britannica.com/science/lymphatic-system.
40. Ruddle NH, Akirav EM. Secondary lymphoid organs: responding to genetic and environmental cues in ontogeny and the immune response. J Immunol. 2009;183(4):2205-12.
41. Green J. WHAT IS LYMPHATIC CIRCULATION: Tactile Medical; 2023 [Available from: https://tactilemedical.com/resource-hub/general/what-is-lymphatic-circulation/#pxMainContent.
42. Jiang X, Nicolls MR, Tian W, Rockson SG. Lymphatic Dysfunction, Leukotrienes, and Lymphedema. Annu Rev Physiol. 2018;80:49-70.
43. Lucas ED, Tamburini BAJ. Lymph Node Lymphatic Endothelial Cell Expansion and Contraction and the Programming of the Immune Response. Frontiers in Immunology. 2019;10.
44. Zhang F, Zarkada G, Yi S, Eichmann A. Lymphatic Endothelial Cell Junctions: Molecular Regulation in Physiology and Diseases. Frontiers in Physiology. 2020;11.
45. Baluk P, McDonald DM. Buttons and Zippers: Endothelial Junctions in Lymphatic Vessels. Cold Spring Harb Perspect Med. 2022;12(12).
46. Jiang X, Nicolls MR, Tian W, Rockson SG. Lymphatic Dysfunction, Leukotrienes, and Lymphedema. Annu Rev Physiol. 2018;80:49-70. Figure 2, Schematic diagram of the lymphatic vascular tree.
47. Krishnamurty AT, Turley SJ. Lymph node stromal cells: cartographers of the immune system. Nature Immunology. 2020;21(4):369-80.
48. Yuan Y, Arcucci V, Levy SM, Achen MG. Modulation of Immunity by Lymphatic Dysfunction in Lymphedema. Front Immunol. 2019;10:76.
49. Aldrich MB, Rasmussen JC, Fife CE, Shaitelman SF, Sevick-Muraca EM. The Development and Treatment of Lymphatic Dysfunction in Cancer Patients and Survivors. Cancers (Basel). 2020;12(8).
50. Christiansen A, Detmar M. Lymphangiogenesis and cancer. Genes Cancer. 2011;2(12):1146-58.
51. La Mendola D, Trincavelli ML, Martini C. Angiogenesis in Disease. Int J Mol Sci. 2022;23(18).
52. Alitalo K, Carmeliet P. Molecular mechanisms of lymphangiogenesis in health and disease. Cancer Cell. 2002;1(3):219-27.
53. Pansky B. Development of The Lymphatic System: LifeMap Sciences; 1982 [Available from: https://discovery.lifemapsc.com/library/review-of-medical-embryology/chapter-128-development-of-the-lymphatic-system.
54. Vaahtomeri K, Karaman S, Mäkinen T, Alitalo K. Lymphangiogenesis guidance by paracrine and pericellular factors. Genes Dev. 2017;31(16):1615-34.
55. Biron-Andreani C, Sleeman JP, Munschauer CE, editors. Understanding the mechanisms of lymphangiogenesis : Page 99 a hope for cancer therapy ?2010.
56. Siemerink MJ, Klaassen I, Van Noorden CJ, Schlingemann RO. Endothelial tip cells in ocular angiogenesis: potential target for anti-angiogenesis therapy. J Histochem Cytochem. 2013;61(2):101-15.
57. Nehls V, Herrmann R. The configuration of fibrin clots determines capillary morphogenesis and endothelial cell migration. Microvasc Res. 1996;51(3):347-64.
58. Bui K, Hong YK. Ras Pathways on Prox1 and Lymphangiogenesis: Insights for Therapeutics. Front Cardiovasc Med. 2020;7:597374.
59. Bekisz S, Baudin L, Buntinx F, Noël A, Geris L. In Vitro, In Vivo, and In Silico Models of Lymphangiogenesis in Solid Malignancies. Cancers (Basel). 2022;14(6).

60. Cho Y, Na K, Jun Y, Won J, Yang JH. Three-Dimensional In Vitro Lymphangiogenesis Model in Tumor Microenvironment. Frontiers in Bioengineering and Biotechnology. 2021;9:697657.
61. Sigma-Aldrich. Cell Viability and Proliferation Assays: Merck; 2024 [Available from: https://www.sigmaaldrich.com/NO/en/technical-documents/technical-article/cell-culture-and-cell-culture-analysis/imaging-analysis-and-live-cell-imaging/cell-viability-and-proliferation
62. Fang IJ, Trewyn BG. Chapter three - Application of Mesoporous Silica Nanoparticles in Intracellular Delivery of Molecules and Proteins. In: Düzgüneş N, editor. Methods in Enzymology. 508: Academic Press; 2012. p. 41-59.
63. Mayr C, Beyreis M, Dobias H, Gaisberger M, Pichler M, Ritter M, et al. Miniaturization of the Clonogenic Assay Using Confluence Measurement. Int J Mol Sci. 2018;19(3).
64. VWR. VWR®, Cellekulturplater med flere brønner. VWR; 2024.
65. Ildikó B, Dániel N, Ferenc F, Judit V, Gábor V, Pálma F, et al. Role of Cytotoxicity Experiments in Pharmaceutical Development. In: Tülay Aşkin Ç, editor. Cytotoxicity. Rijeka: IntechOpen; 2017. p. Ch. 8.
66. NanoEnTek. 2 Channel C-Chip: Cambridge Bioscience; 2024 [Available from: https://www.bioscience.co.uk/product~777707.
67. Morten BC, Scott RJ, Avery-Kiejda KA. Comparison of Three Different Methods for Determining Cell Proliferation in Breast Cancer Cell Lines. J Vis Exp. 2016(115).
68. Staton CA, Reed MW, Brown NJ. A critical analysis of current in vitro and in vivo angiogenesis assays. Int J Exp Pathol. 2009;90(3):195-221.
69. Dietrich F, Lelkes PI. Fine-tuning of a three-dimensional microcarrier-based angiogenesis assay for the analysis of endothelial-mesenchymal cell co-cultures in fibrin and collagen gels. Angiogenesis. 2006;9(3):111-25.
70. Nakatsu M, Davis J, Hughes C. Optimized Fibrin Gel Bead Assay for the Study of Angiogenesis. Journal of visualized experiments : JoVE. 2007;3:186.
71. Carpentier G, Berndt S, Ferratge S, Rasband W, Cuendet M, Uzan G, Albanese P. Angiogenesis Analyzer for ImageJ — A comparative morphometric analysis of “Endothelial Tube Formation Assay” and “Fibrin Bead Assay”. Scientific Reports. 2020;10(1):11568.
72. Unterleuthner D, Kramer N, Pudelko K, Burian A, Hengstschläger M, Dolznig H. An Optimized 3D Coculture Assay for Preclinical Testing of Pro- and Antiangiogenic Drugs. SLAS DISCOVERY: Advancing the Science of Drug Discovery. 2017;22(5):602-13.
73. Nakatsu MN, Davis J, Hughes CC. Optimized fibrin gel bead assay for the study of angiogenesis. J Vis Exp. 2007(3):186.
74. Jutte LS, Knight KL, Long BC, Hawkins JR, Schulthies SS, Dalley EB. The uncertainty (validity and reliability) of three electrothermometers in therapeutic modality research. J Athl Train. 2005;40(3):207-10.
75. Yun C, Kim SH, Kim KM, Yang MH, Byun MR, Kim J-H, et al. Advantages of Using 3D Spheroid Culture Systems in Toxicological and Pharmacological Assessment for Osteogenesis Research. International Journal of Molecular Sciences. 2024;25(5):2512.
76. Yuan Y, Arcucci V, Levy S, Achen M. Modulation of Immunity by Lymphatic Dysfunction in Lymphedema. Frontiers in Immunology. 2019;10.
77. Kim A, Park S, Sung JH. Cell Viability and Immune Response to Low Concentrations of Nickel and Cadmium: An In Vitro Model. Int J Environ Res Public Health. 2020;17(24).
78. Nexelcom. Sources of Hemacytometer Counting Errors: Nexelcom; 2024 [Available from: https://www.nexcelom.com/applications/cellometer/cell-counting/counting-errors/.
79. Bodiou V, Moutsatsou P, Post MJ. Microcarriers for Upscaling Cultured Meat Production. Front Nutr. 2020;7:10.
80. Kim JS, Nam MH, An SS, Lim CS, Hur DS, Chung C, Chang JK. Comparison of the automated fluorescence microscopic viability test with the conventional and flow cytometry methods. J Clin Lab Anal. 2011;25(2):90-4.

Appendix

A.1. Cell Counting

Table 1. Cell counting of the control group with hemocytometer, proliferation assay.

Cell counting of the control group with hemocytometer														
	Viable cells in each well							Non-viable cells in each well						
Square	1	2	3	4	5	6	Average	1	2	3	4	5	6	Average
1	2	11	14	0	2	31		0	9	2	0	3	11	
2	5	31	5	8	13	30		7	20	2	2	10	7	
3	26	5	11	3	16	17		19	2	3	4	5	15	
4	10	8	2	0	4	35		12	7	3	5	7	19	
5	5	11	6	0	9	26		7	5	6	4	3	4	
Average	9.6	13.2	7.6	2.2	8.8	27.8	11.53	9	8.6	3.2	3	5.6	11.2	6.77

Table 2. Cell counting of the 10 μM Cd^{2+} group with hemocytometer, proliferation assay.

Cell counting of the 10 μM Cd^{2+} group with hemocytometer														
	Viable cells in each well							Non-viable cells in each well						
Square	1	2	3	4	5	6	Average	1	2	3	4	5	6	Average
1	2	3	5	1	2	3		2	17	24	7	3	17	
2	9	9	2	2	0	0		7	26	13	8	15	7	
3	6	8	2	2	5	2		6	7	9	7	6	8	
4	4	8	4	0	2	1		2	25	12	8	4	9	
5	2	4	3	3	1	0		19	9	7	8	11	2	
Average	4.6	6.4	3.2	1.6	2	1.2	3.17	7.2	16.8	13	7.6	7.8	8.6	10.17

Table 3. Cell counting of the 20 μM Cd2+ group with hemocytometer, proliferation assay.

Cell counting of 20 μM Cd^{2+} group with hemocytometer														
	Viable cells in each well							Non-viable cells in each well						
Square	1	2	3	4	5	6	Average	1	2	3	4	5	6	Average
1	6	4	15	0	7	3		1	5	15	11	20	7	
2	10	14	0	3	14	6		12	15	21	15	11	4	
3	1	4	7	0	1	1		15	7	20	18	23	21	
4	1	3	0	3	4	0		9	17	11	18	25	12	
5	0	5	11	5	2	0		12	14	5	13	16	45	
Average	3.6	6	6.6	2.2	5.6	2	4.30	9.8	11.6	14.4	15	19	17.8	14.60

A.2. MCs and Sprouts

Table 4. Raw data of MCs and sprouts for the control group on day 4.

Control group day 4			
Well	MCs	Sprouts	Sprout/MC
2A	118	123	1.04
2B	62	97	1.57
2C	57	89	1.56
2D	17	34	2.00
3A	36	99	2.75
3B	50	70	1.40
3C	32	53	1.66
3D	36	88	2.44
4A	90	117	1.30
4B	94	111	1.18
4C	17	56	3.29
4D	28	72	2.57
Average	53.08	84.08	1.90

Table 5. Raw data of MCs and sprouts for the 10 µM Cd group on day 4.

10 µM Cd group			
Well	MCs	Sprouts	Sprouts/MC
2A	11	0	0
2B	2	0	0
2C	2	0	0
2D	8	0	0
3A	5	0	0
3B	5	0	0
3C	0	0	0
4A	11	0	0
4B	12	0	0
4C	2	0	0
Average	5.8	0	0

Table 6. Raw data of MCs and sprouts for the 20 µM Cd group on day 4.

20 µM Cd group			
Well	MCs	Sprouts	Sprouts/MC
2A	14	13	0.93
2B	13	6	0.46
2C	10	0	0.00
2D	8	8	1.00
3A	14	10	0.71
3B	7	5	0.71
3C	4	0	0.00
4A	8	7	0.88
4B	4	8	2.00
4C	3	0	0.00
Average	8.5	5.7	0.67

A.3. Calculations

A.3.1. Volumes and Formulas

Volume of cells in each well: 1 ml

Volume of cells: 100 µL

Volume of Trypan blue: 100 µL

Cells/ml = Cells (avg. from hemocytometer) * dilution factor * 10^4 (volume factor)

Dilution factor: $\frac{Total\ volume}{Volume\ of\ cells} = \frac{200\ \mu L}{100\ \mu L} = 2$

A.3.2. Proliferation Assay

A.3.2.1. Control Group:

Viable cells: 11.53 * 2 * 10^4 = 230 600 cells/ml * 1 ml = 230 600 cells

Non-viable cells: 6.77 * 2 * 10^4 = 135 400 cells/ml * 1ml = 135 400 cells

Total cells: 230 600 + 135 400 = 366 000 cells

% Viable cells = $\frac{230\ 600}{366\ 000} \cdot 100$ = 63.01%

A.3.2.2. 10 µM Cd Group:

Viable cells: 3.17 * 2 * 10^4 = 63 400 cells/ml * 1 ml = 63 400 cells

Non-viable cells: 10.17 * 2 * 10^4 = 203 400 cells/ml * 1ml = 203 400 cells

Total cells: 63 400 + 203 400 = 266 800 cells

% Viable cells = $\frac{63\ 400}{266\ 800} \cdot 100$ = 23.76%

A.3.2.3. 20 µM Cd Group:

Viable cells: 4.3 * 2 * 10^4 = 86 000 cells/ml * 1 ml = 86 000 cells

Non-viable cells: 14.6 * 2 * 10^4 = 203 400 cells/ml * 1ml = 292 000 cells

Total cells: 86 000 + 292 000 = 378 000 cells

% Viable cells = $\frac{86\ 000}{378\ 000} \cdot 100$ = 22.75%

A.3.3. Cells/ml in T-75 Flask (HMVEC-dLyAd P8)

Table 7. Raw data of cell counting from T-75 flask (HMVEC-dLyAd P8).

Cell counting of HMVEC-dLyAd P8	
Square	Cells
1	55
2	38
3	44
4	69
5	45
Average	50.2

Cells/ml: $50.2 * 10^4 = \underline{502\ 000}$

Wanted approximately 25 000 cells/well, therefore required volume of cell suspension is:

3 plates * 6 * wells = 18

18 * 25 000 cells = 450 000 cells

Volume of cell suspension: $\frac{450\ 000\ cells}{502\ 000 ml} = \underline{0.9\ ml}$

Non-uniform distribution of cells resulted in fewer cells in some of the wells in the 10 µM group.

A.3.3.1. Hypothetical Calculation of mol Cd/cell if Cell Distribution were ± 15 000 cells:

^{n}Cd 10 µM: $10 * 10^{-6}$ mol/L * 0.002 L = $\underline{2 * 10^{-8}\ mol}$

^{n}Cd 20 µM: $20 * 10^{-6}$ mol/L * 0.002 L = $\underline{4 * 10^{-8}\ mol}$

^{n}Cd/cell 10 µM: $\frac{2 \cdot 10^{-8}\ mol}{10\ 000\ cells} = \underline{2 * 10^{-12}\ mol/cell}$

^{n}Cd/cell 20 µM: $\frac{4 \cdot 10^{-8}\ mol}{40\ 000\ cells} = \underline{1 * 10^{-12}\ mol/cell}$

A.4. Python Scripts

```python
# -*- coding: utf-8 -*-
"""
Created on Wed Apr 24 16:34:57 2024

@author: trymj
"""

import numpy as np
import matplotlib.pyplot as plt

control = np.array([9.6, 13.2, 7.6, 2.2, 8.8, 27.8])
ten_micromolar = np.array([4.6, 6.4, 3.2, 1.6, 2, 1.2])
twenty_micromolar = np.array([3.6, 6, 6.6, 2.2, 5.6, 2])

average_control = np.mean(control)
average_ten_micromolar = np.mean(ten_micromolar)
average_twenty_micromolar = np.mean(twenty_micromolar)

number_of_cells_control = average_control * 2 * (10**4)
number_of_cells_ten_micromolar = average_ten_micromolar * 2 * (10**4)
number_of_cells_twenty_micromolar = average_twenty_micromolar * 2 * (10**4)

normalized_control = number_of_cells_control / number_of_cells_control
normalized_10 = number_of_cells_ten_micromolar / number_of_cells_control
normalized_20 = number_of_cells_twenty_micromolar / number_of_cells_control

std_control = (np.std(control)* 2 * (10**4))/number_of_cells_control
std_ten_micromolar = (np.std(ten_micromolar)* 2 * (10**4))/number_of_cells_control
std_twenty_micromolar = (np.std(twenty_micromolar)* 2 * (10**4))/number_of_cells_control

day_0 = 25000/number_of_cells_control

fig, ax = plt.subplots()
bars = ax.bar(
    ['Control', '10 µM Cd', '20 µM Cd'],
    [normalized_control, normalized_10, normalized_20],
    yerr=[std_control, std_ten_micromolar, std_twenty_micromolar],
    color=['maroon', 'darkorchid', 'purple'],
    capsize=5
)

ax.axhline(y=day_0, color='black', linestyle='--', linewidth=1, label='Day 0 (25,000 cells)')
ax.legend()

ax.set_ylabel('Normalized number of cells')
ax.set_title('Average number of viable cells in each well on day 3')
plt.show()
```

Figure 22. Python script of Figure 13.

```python
# -*- coding: utf-8 -*-
"""
Created on Tue Apr 23 16:55:12 2024

@author: trymj
"""

# -*- coding: utf-8 -*-
"""
Created on Tue Apr 23 16:19:45 2024

@author: trymj
"""
import numpy as np
import matplotlib.pyplot as plt

control = np.array([9, 8.6, 3.2, 3, 5.6, 11.2])
ten_micromolar = np.array([7.2, 16.8, 13, 7.6, 7.8, 8.6])
twenty_micromolar = np.array([9.8, 11.6, 14.4, 15, 19, 17.8])

average_control = np.mean(control)
average_ten_micromolar = np.mean(ten_micromolar)
average_twenty_micromolar = np.mean(twenty_micromolar)

number_of_cells_control = average_control * 2 * (10**4)
number_of_cells_ten_micromolar = average_ten_micromolar * 2 * (10**4)
number_of_cells_twenty_micromolar = average_twenty_micromolar * 2 * (10**4)

normalized_control = number_of_cells_control / number_of_cells_control
normalized_10 = number_of_cells_ten_micromolar / number_of_cells_control
normalized_20 = number_of_cells_twenty_micromolar / number_of_cells_control

std_control = (np.std(control)* 2 * (10**4))/number_of_cells_control
std_ten_micromolar = (np.std(ten_micromolar)* 2 * (10**4))/number_of_cells_control
std_twenty_micromolar = (np.std(twenty_micromolar)* 2 * (10**4))/number_of_cells_control

day_0 = 25000/number_of_cells_control

fig, ax = plt.subplots()
bars = ax.bar(
    ['Control', '10 µM Cd', '20 µM Cd'],
    [normalized_control, normalized_10, normalized_20],
    yerr=[std_control, std_ten_micromolar, std_twenty_micromolar],
    color=['maroon', 'darkorchid', 'purple'],
    capsize=5
)

ax.set_ylabel('Normalized number of cells')
ax.set_title('Average number of non-viable cells in each well on day 3')
ax.axhline(y=day_0, color='black', linestyle='--', linewidth=1, label='Day 0 (25,000 cells)')
ax.legend()
plt.show()
```

Figure 23. Python script for Figure 14.

```python
# -*- coding: utf-8 -*-
"""
Created on Tue Apr 23 17:05:46 2024

@author: trymj
"""

import numpy as np
import matplotlib.pyplot as plt

sprouts_per_bead_control = np.array([1.04, 1.57, 1.56, 2.0, 2.75, 1.4, 1.66, 2.44, 1.3, 1.18, 3.29, 2.57])
sprouts_per_bead_ten = np.array([0, 0, 0, 0, 0, 0, 0, 0, 0, 0])
sprouts_per_bead_twenty = np.array([0.93, 0.46, 0, 1, 0.71, 0.71, 0, 0.88, 2, 0])

mean_control = np.mean(sprouts_per_bead_control)
mean_ten = np.mean(sprouts_per_bead_ten)
mean_twenty = np.mean(sprouts_per_bead_twenty)

std_control = np.std(sprouts_per_bead_control)
std_ten = np.std(sprouts_per_bead_ten)
std_twenty = np.std(sprouts_per_bead_twenty)

labels = ['Control', '10 μM CdCl$_2$', '20 μM CdCl$_2$']
means = [mean_control, mean_ten, mean_twenty]
std_devs = [std_control, std_ten, std_twenty]

fig, ax = plt.subplots()
bars = ax.bar(
    labels,
    means,
    yerr=std_devs,
    color=['maroon', 'darkorchid', 'purple'],
    capsize=5
)

ax.set_ylabel('Sprouts/MC')
ax.set_title('Average Sprouts/MC on Day 4')

plt.show()
```

Figure 24. Python script of Figure 20.